

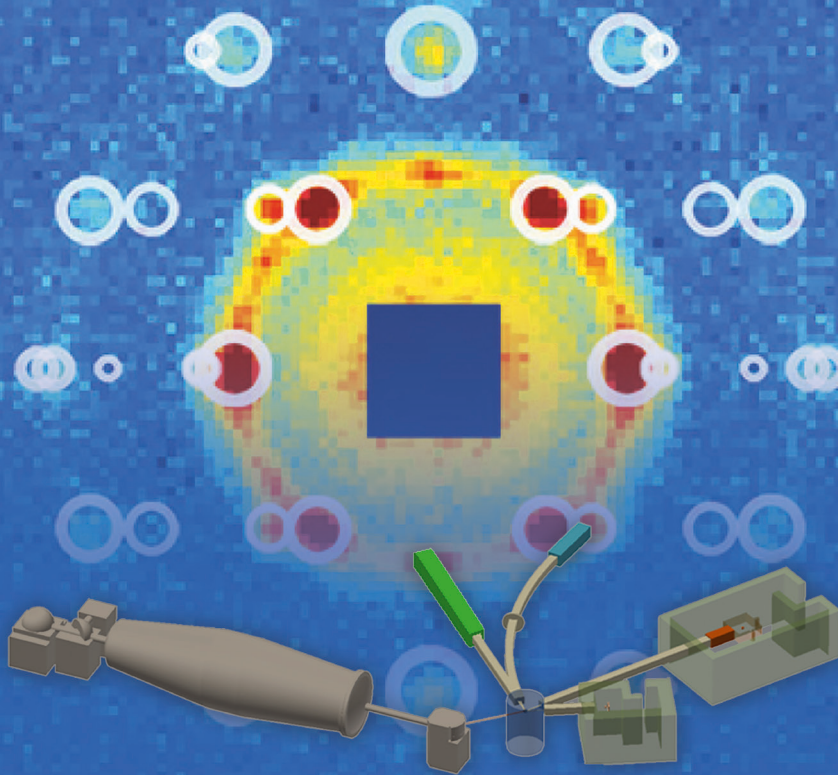
Conceptual Design Report

NOVA ERA (Neutrons Obtained Via Accelerator
for Education and Research Activities)

A Jülich High Brilliance Neutron Source project



Eric Mauerhofer, Ulrich Rücker, Tobias Cronert, Paul Zakalek, Johannes Baggemann,
Paul-Emmanuel Doege, Jingjing Li, Sarah Böhm, Harald Kleines, Thomas Gutberlet,
and Thomas Brückel



Allgemeines /
General
Band / Volume 7
ISBN 978-3-95806-280-1



Forschungszentrum Jülich GmbH
Jülich Centre for Neutron Science
JCNS

Conceptual Design Report

**NOVA ERA (Neutrons Obtained Via Accelerator for
Education and Research Activities)**

A Jülich High Brilliance Neutron Source project

Eric Mauerhofer, Ulrich Rücker, Tobias Cronert, Paul Zakalek,
Johannes Baggemann, Paul-Emmanuel Doege, Jingjing Li,
Sarah Böhm, Harald Kleines, Thomas Gutberlet, and Thomas Brückel

Schriften des Forschungszentrums Jülich
Reihe Allgemeines / General

Band / Volume 7

ISSN 1433-5565

ISBN 978-3-95806-280-1

Bibliographic information published by the Deutsche Nationalbibliothek.
The Deutsche Nationalbibliothek lists this publication in the Deutsche
Nationalbibliografie; detailed bibliographic data are available in the
Internet at <http://dnb.d-nb.de>.

Publisher and
Distributor: Forschungszentrum Jülich GmbH
Zentralbibliothek
52425 Jülich
Tel: +49 2461 61-5368
Fax: +49 2461 61-6103
Email: zb-publikation@fz-juelich.de
www.fz-juelich.de/zb

Cover Design: Grafische Medien, Forschungszentrum Jülich GmbH

Printer: Grafische Medien, Forschungszentrum Jülich GmbH

Copyright: Forschungszentrum Jülich 2017

Schriften des Forschungszentrums Jülich
Reihe Allgemeines / General, Band / Volume 7

ISSN 1433-5565
ISBN 978-3-95806-280-1

The complete volume is freely available on the Internet on the Jülicher Open Access Server (JuSER)
at www.fz-juelich.de/zb/openaccess.



This is an Open Access publication distributed under the terms of the [Creative Commons Attribution License 4.0](https://creativecommons.org/licenses/by/4.0/),
which permits unrestricted use, distribution, and reproduction in any medium, provided the original work is properly cited.

Acknowledgements

For the preparation of this report we kindly acknowledge the support and valuable discussions by R. Nabbi and J.P. Dabruck of RWTH Aachen regarding neutronic calculations and of M. Klaus of TU Dresden regarding development and construction of cold moderators and mixing cryostats and C. Lange for support with the experimental validation at the AKR-2 reactor at TU Dresden.

Content

EXECUTIVE SUMMARY	4
INTRODUCTION	5
0. FOREWORD	6
1. RATIONALE	7
1.1 NEUTRON PROVISION	8
1.2 HIGH BRILLIANCE ACCELERATOR DRIVEN NEUTRON SOURCES	9
1.3 BASELINE DESIGN	10
2. NEUTRONS TO USERS	11
2.1. CHEMISTRY AND MATERIAL SCIENCE.....	11
2.2. MAGNETISM AND MAGNETIC MATERIALS.....	12
2.3. ENGINEERING	12
2.4. SOFT MATTER AND BIOLOGY	13
2.5 CULTURAL HERITAGE	14
2.6 EDUCATION AND TRAINING	14
2.7 INDUSTRY, METHOD DEVELOPMENT	15
3. CONCEPTUAL DESIGN OF THE NEUTRON SOURCE	16
3.1 ACCELERATOR, ION SOURCE	16
3.3 MODERATOR REFLECTOR ASSEMBLY	23
3.4 SOURCE PERFORMANCE	25
3.5 COLD MODERATOR.....	30
3.6 BIOLOGICAL SHIELDING.....	32
4. INSTRUMENTS	35
4.1 PROMPT AND DELAYED GAMMA NEUTRON ACTIVATION ANALYSIS.....	35
4.2 NEUTRON IMAGING.....	37
4.3 NEUTRON REFLECTOMETRY	38
4.4 SMALL ANGLE NEUTRON SCATTERING	39
4.5 NEUTRON POWDER DIFFRACTION	41
5. SAFETY	43
6. CONTROL SYSTEMS	44
6.1 NOVA ERA CONTROL SYSTEM	44
6.2 INSTRUMENT CONTROL SYSTEMS	45
7. HANDLING OF RADIOACTIVE COMPONENTS	47
8. INFRASTRUCTURE	50
9. COSTING	51
10. SUMMARY	52
11. REFERENCES	53
<i>Appendix 1</i> <i>Benchmark for neutron emission from beryllium target</i>	<i>55</i>
<i>Appendix 2</i> <i>Proton reactions on beryllium and vanadium with energy thresholds lower than 13 MeV..</i>	<i>57</i>
<i>Appendix 3</i> <i>Time structure, full widths at half maximum and die-away times of neutron pulses obtained for the different neutron</i>	<i>58</i>
<i>Appendix 4</i> <i>Brilliance for the neutron channels</i>	<i>60</i>
<i>Appendix 5</i> <i>Excerpt (summarised) of the German radiation ordinance (StrlSchV) for installation and operation of a facility producing ionizing radiation</i>	<i>62</i>
<i>Appendix 6</i> <i>Activity calculations</i>	<i>64</i>

Executive Summary

Neutron scattering has proven to be one of the most powerful methods for the investigation of structure and dynamics of condensed matter on atomic length and time scales. A severe drawback in using neutrons is the limited possibility to access neutrons offered at nuclear research reactors or accelerator driven spallation sources, which are costly to build and to operate. To offer neutrons accessible more easily for science, training, and industrial use is a challenge. The concept of a compact accelerator based neutron source is a new approach to tackle this challenge with the aim to bring neutrons to the users on demand and in a cost effective way. Such a facility can be operated within the staff constraints of a university or an industrial R&D laboratory.

Compact accelerator based neutron sources (CANS) produce neutrons by the nuclear reaction between a low energy proton beam and light elements as beryllium or lithium. Depending on the power of the accelerator and the number of target stations and instruments such a source can be equivalent to small and medium flux reactor or spallation based neutron sources. With the aim to design CANS to be operated at universities, research institutes or industry laboratories a conceptual design report is presented for a small neutron source named NOVA ERA (Neutrons Obtained Via Accelerator for Education and Research Activities). Such a neutron source can be built at low cost with low maintenance efforts and without nuclear licencing procedure as small accelerator facility. Main features of this new concept can be summarised as follows:

- NOVA ERA consists of a low power proton accelerator. The proton beam is hitting a target of Be releasing neutrons which are moderated by thermal or cold (cryogenic) moderators. The moderated neutron beams are transferred by neutron guides and neutron optical devices to corresponding instruments e.g. an imaging station, diffractometer or reflectometer.
- Basic parameters of the NOVA ERA neutron source described in this conceptual design report are:
 - 5 MeV electrostatic tandem accelerator producing a pulsed proton beam of 10 MeV at 1 mA peak current and an average power of 400 W
 - Be target with peak neutron yield of $2 \cdot 10^{13} \text{ s}^{-1}$
 - Cold and thermal moderators with biological shielding
 - Up to 6 neutron channels for serving various instruments as e.g. imaging station, reflectometer, small angle neutron scattering diffractometer, neutron powder diffractometer, prompt gamma neutron activation analysis. The neutron flux calculated at the sample position of such instruments is in the range of the flux at small reactor neutron sources. The disadvantage of such a low flux is compensated by the easy access and availability of the source which allow longer measurement times.
 - The costs for the accelerator, target station, neutron moderators and a basic set of instruments are approximately 10 M EUR.

Introduction

Neutron scattering is an important analytical tool to study structure and dynamics of matter in all areas of science and technology, e.g. physics, chemistry, biophysics, material science, cultural heritage and medicine. A severe drawback in using neutrons is the limited access of nuclear research reactors or accelerator driven spallation sources. These large scale facilities are costly to build and to operate. This restricts the number of neutron sources available and increases the user pressure on these sources. An alternative option to provide and exploit neutrons can be the use of nuclear reactions with relatively small low energy proton accelerators.

These compact accelerator-driven neutron sources, or CANS, can serve efficiently many of the needs that were hitherto covered by small reactors or spallation sources. In addition, compact accelerator based neutron sources using low-energy nuclear reactions could be implemented at universities, research centres or industry labs allowing direct access to neutron methods. The conceptual design of such a neutron source as a facility for education and research called NOVA ERA is presented in this report. Describing the means for the provision of neutrons and the current state-of-the-art of compact accelerator based neutron sources, a baseline design of the NOVA ERA concept is provided. A description is given of the scientific relevance and potential in major scientific areas, as well as for education purposes and for industry.

The conceptual design with all relevant components of such a source as ion source and accelerator, target assembly, moderators, source performance and selected instrumentation is described in detail. Basic technical parameters and performances are specified. Radiation safety, biological shielding, general aspects of safety, required control and operation systems are described. The necessary infrastructure to build and operate this neutron source is outlined as well as requirements dealing with handling of radioactive components and other regulatory aspects in this context. An estimation of the costing to build and operate a NOVA ERA neutron source is provided.

The conceptual design report (CDR) presented here provides a substantial guideline to define the construction, realization and operation of a compact accelerator based neutron source at universities or research laboratories. NOVA ERA allows one to provide and exploit a versatile neutron source with high potential for basic investigations using neutrons in science, education and industry beyond existing large-scale neutron facilities. NOVA ERA type sources enable the efficient access to neutrons and thus open up the opportunity to use neutrons at universities at local or regional level.

0. Foreword

This document provides a conceptual design report for a low cost but efficient small-scale neutron facility which enables the basic, most important diffraction and analysis techniques to be performed locally, without the need to access a large-scale facility. Such a source, suitable as central facility for universities, companies, or museums, could have a large regional impact by “bringing neutrons to users” instead of “bringing users to neutrons”, as is the case for present day large scale neutron facilities.

Technological advances are the basis for economic development. This is true in many areas ranging from microelectronics and engineered materials to advanced pharmaceuticals and medical devices. Neutron based analytical techniques have a substantial impact on a wide range of fields in advanced science and engineering, new technologies and health.

Neutrons can provide unique information on the reaction dynamics of complex biomolecular systems and enzymatic reactions, on the structure and dynamics in novel materials and nanocomposites, or for the visualization of processes or artefacts in engineering devices or cultural heritage objects, complementing analytical techniques such as electron microscopy, X-rays or NMR. Emerging communities do not exploit neutrons to their full capacity due to the fact that useful neutron beams can only be generated at research reactors and/or high energy neutron spallation sources. These are overloaded by demand and typically several months of preparation are required before beam time is provided.

Small to medium power neutron sources could provide a network of facilities that offers an invaluable experimental resource, which also serves for the development of the technique and for the training of the community. Not all measurements or experiments require the beam intensity offered by high flux neutron sources, and excellent science programs can be carried out at smaller facilities. The science programs carried out at smaller sources may be adapted to specialised communities, which may better reflect local or regional requirements. The use of such facilities will certainly not be restricted to neutron scattering experiments. Scientific and technological experience and know-how developed at such sources can be shared efficiently with the larger facilities.

Recent developments in accelerator technology have made it possible to produce useful neutron fluxes at accelerator based facilities suitable for universities and industrial laboratories. In addition to basic research, these alternative neutron sources will be important for educational and training purposes. They will also offer a platform for method development. In a wider perspective, this technology should make it possible to introduce neutron research and applications to industrial and national research centres at local and regional scale which, at present, have no access to large scale neutron sources.

This document presents the scientific case and the conceptual design for a new experimental facility, NOVA ERA (Neutrons Obtained Via Accelerator for Education and Research Activities). The facility will enable excellent research with pulsed and continuous neutron beams to be performed in the next decades and will provide novel means to investigate and understand matter, because it will enable to use neutron methods close to any laboratory sites. A demonstrator of this kind of facility shall be built at Forschungszentrum Jülich to demonstrate the capabilities to provide integrated access to a multitude of analytical methods for science and industry.

1. Rationale

Neutron scattering has proven to be one of the most powerful methods for the investigation of condensed matter on atomic length and time scales. This is due to the fact that the neutron's energy matches the energy scale of atomic and molecular motions and of spin excitations, whereas the neutron's wavelength is on the same order of magnitude as the typical length scales in condensed matter systems. However, many applications of neutron spectroscopy are flux limited and therefore any new generation of neutron source has boosted the development of new instrumentation. With the construction of the ESS (European Spallation Source), the European neutron user community is looking forward to the brightest neutron source worldwide. At the same time there is an ongoing concentration of neutron science to only a few neutron facilities. These "bright lighthouses" serve the needs of a limited amount of experienced researchers, but the smaller or medium flux sources used for method development, user recruitment, education, proof-of-principle experiments or bare capacity are vanishing [1].

Compact accelerator-driven neutron sources with high brilliance neutron provision present an alternative to nuclear reactor and spallation based neutron sources to provide scientists and industry with the required neutrons to probe the structure and dynamics of matter in many areas of science. These include physics, chemistry, magnetism and superconductivity, material sciences, cultural heritage, biology, soft matter, health, and environmental and climate science.

The Jülich Centre for Neutron Science has started a project for such compact accelerator-driven neutron sources CANS. Such sources will be able to replace the network of aging reactor based sources in Europe. They will offer direct and easy access to neutrons for science and industry. The concept aims for a compact neutron source as an efficient and cost effective alternative to the current low- and medium-flux reactor and spallation sources. Such CANS are scalable and reach from high-end competitive medium size neutron facilities to small local or regional sources adapted at the need of the operating team. The technical design report for a top-tier facility, named HBS for High Brilliance Neutron Source [2], will be given elsewhere. Here we focus on NOVA ERA (Neutrons Obtained Via Accelerator for Education and Research Activities), a novel type of small, local, flexible and multipurpose neutron laboratory, where a compact neutron production and moderator system provides thermal and cold neutrons with high brilliance efficiently extracted in an optimised neutron transport system. Shaping the experiment from the detector to the source, basic neutron experiments will allow fulfilling the specific scientific requirements in a flexible and efficient way for the neutron user.

NOVA ERA aims for basic applications of neutrons, such as neutron imaging, small angle neutron scattering, reflectometry, diffraction or prompt gamma activation analysis. These techniques should become available for neutron laboratories at universities, engineering or industry based research environments. The basic design, neutron provision, technical realisation and cost effectiveness is presented in this report. It presents an overview on all technical and administrative aspects to realise such a laboratory oriented neutron source and can be used to develop specific projects along this line.

1.1 Neutron provision

Processes to produce neutrons are fission in research reactors, spallation using high-power proton accelerators, and nuclear reactions with low-energy proton accelerators [3]. Furthermore, fusion of deuterium with deuterium or tritium in solid targets is used in small portable neutron generators, however, with very low neutron yields. Neutrons may be produced also by photodisintegration using high-energy gamma rays or Bremsstrahlung radiation. Main features of each process are as follows:

- Research reactors produce neutrons by a chain reaction of nuclear fissions. Each fission process produces on average about 1 useable neutron with a heat release of 180 MeV per neutron. High flux research reactors as the FRM II in Garching, Germany, or the ILL in Grenoble, France, apply highly enriched uranium to offer a neutron flux around $10^{15} \text{ s}^{-1} \text{ cm}^{-2}$.
- Spallation neutron sources use (pulsed) proton beams in the GeV range to hit a heavy metal target (e.g. lead, tungsten, mercury, or uranium), where around 20 to 30 neutrons per proton are produced with a heat release ranging between 30 and 50 MeV per neutron. The high neutron yield combined with the relatively small heat release makes spallation an ideal choice for a source optimised for high source strength. However, the proton/target interaction zone is elongated to several 10 cm due to the high energy of the protons which hampers coupling the neutrons efficiently into a compact moderator. The high radiation level requires massive shielding and a minimum distance of optical elements from the moderator.
- Nuclear reactions with light target elements such as lithium or beryllium produce neutrons by bombardment of the target material with low or medium energy protons or deuterons in the range of 2 to 50 MeV. The neutron yield is around 10^{-2} per proton (or per deuteron) with a heat release of around 1,000 MeV per neutron.
- Fusion (deuterium-tritium in solid target) is used for small portable neutron generators. However, only low neutron yields of $4 \cdot 10^{-5}$ neutrons per 400 keV deuteron with a heat release of 10,000 MeV per neutron can be achieved.
- Electrons with energies between 10 MeV and 100 MeV are used to generate neutrons via Bremsstrahlung and the nuclear photo effect in the "giant dipole resonance" (GDR) region with similar efficiencies than the processes based on nuclear reactions with protons or deuterons. This process is associated with a high background of high-energy gamma radiation.

The first two techniques are used very successfully in Europe in a suite of national and international neutron facilities and offer the highest neutron flux production with versatile options. The third technique for obtaining high-brilliance neutrons based on low-energy proton accelerators has been considered less for neutron scattering purposes due to the low neutron flux provided. In the US and Japan such sources exist, which, however, are not optimised for scattering and neutron analytics. The University of Bloomington operates the LENS facility [4]. In Japan, the JCANS network of small sources has been established [5].

1.2 High brilliance accelerator driven neutron sources

Despite the reduced neutron flux, accelerator based neutron sources offer a versatile and efficient opportunity to improve and spread access to neutrons and a new route for supplying neutrons with leading research infrastructures directly to science and industry. The neutron production efficiency and the characteristics of the neutron beam generated using low energy ion accelerators considerably depend on the target material and its configuration as well as on the energy of the primary ions, respectively. An overview of existing and planned compact accelerator driven neutron sources was published recently [6]. However, none of these existing sources are optimised for the purposes described in this CDR.

Traditionally, neutron sources are optimised to deliver highest neutron current – or integral flux – in order to be able to serve several different instruments by one moderator. The high brilliance compact accelerator driven neutron source aims at maximizing the brilliance of single neutron beams, where brilliance B is defined as:

$$B = \frac{\text{neutrons}}{\text{s} \cdot \text{cm}^2 \cdot \text{mrad}^2 \cdot 1\% \frac{\Delta\lambda}{\lambda}} \quad (1)$$

The source brilliance is given by the number of neutrons in a wavelength band emitted per second, normalised to the source area and the solid angle into which the neutrons are emitted. B is the relevant quantity for the design of instruments as in conservative neutron optics, B is conserved according to Liouville's theorem.

Following the idea that “no one-fits-all”, the best brilliance for a specific experiment is achieved by an optimised setup starting from a dedicated target-moderator unit for each individual neutron instrument. Thus, the number of neutrons useful for the experiment in question is maximised, minimising the waste associated with neutrons produced but not used in experiments. This concept is based on a compact design of the target and moderator unit combined with sophisticated neutron optics and delivery systems. Such an optimised setup offers a unique and flexible template for individual experimental stations and local facilities. In return, unprecedentedly high neutron brilliance per accelerator power for an instrument is achieved compared to the source flux of existing similar facilities. This offers a new versatile platform and opens the door to variable cost-effective neutron sources.

The present report describes the conceptual and technical design for such an optimised accelerator based neutron source. In 2014, the Jülich Centre for Neutron Science had started to develop and demonstrate the technical and scientific feasibility of such a neutron source to complement and expand the access to neutrons beside reactor and spallation based neutron sources. The source will open up new opportunities and a largely unexplored route beyond the existing large-scale neutron facilities to exploit neutrons. Large universities or research centres will be in a position to host their own neutron source presenting new options within the European Research Area. Being scalable on demand, such a neutron source will be able to be operated on the level of a small university laboratory as described in this report or as an extended research facility for multiple uses by users. The latter, the so-called High Brilliance Source HBS project [2] will be described elsewhere.

1.3 Baseline design

The main components of the NOVA ERA neutron source are the following:

- a 5 MeV electrostatic tandem accelerator producing a pulsed proton beam of 10 MeV at 1 mA peak current and an average power of 400 W,
- a water cooled beryllium (or vanadium) target in an aluminium mounting for production of fast neutrons through the nuclear reactions ${}^9\text{Be}(p,n){}^9\text{B}$ (or ${}^{51}\text{V}(p,n){}^{51}\text{Cr}$)
- a neutron moderator-reflector assembly made of polyethylene and lead to thermalize the fast neutrons,
- a cold moderator using either parahydrogen or solid methane to produce cold neutrons, and
- a biological shielding made of borated polyethylene and lead to reduce neutron and gamma dose rate to an acceptable level.

Components of NOVA ERA are optimised in order to deliver fast, thermal, and cold pulsed neutron beams with properties (energy, time structure, divergence, energy resolution) fitting each instrument's requirements. Based on high current accelerators with pulsed proton or deuteron beam compact neutron sources allow optimised neutron instruments with unprecedented brilliance due to the inclusion of the target-moderator unit as part of the particular instrument design. For this purpose compact small finger-like thermal and cold moderator systems are used to boost the cold neutron brilliance. Developments of cryogenic moderators and tests of such systems have been done in close collaboration with the TU Dresden [7]. A compact target-moderator-reflector station is considered to produce a high neutron yield. Neutronic calculations have shown the parameter space of the target-reflector unit. Concepts for neutron instruments such as reflectometers, small angle neutron scattering instruments, neutron imaging stations, diffractometers or prompt gamma analysing instruments are incorporated.

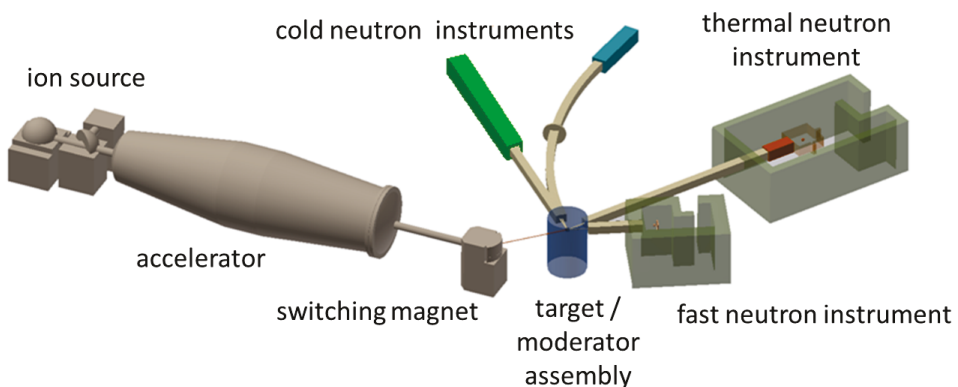


Fig. 1.1. Artistic view of NOVA ERA with four beam-lines and instruments

2. Neutrons to Users

Neutrons are an essential tool in science and industry for probing structure and dynamics of matter from mesoscale to nanoscale and from seconds to nanoseconds. In Europe research benefits from a unique environment of various neutron sources with the flagship facilities ILL in Grenoble, France, MLZ in Garching, Germany, and ESS in Lund, Sweden, which is currently under construction and will represent the world's most powerful neutron facility.

Typical problems in science and industry mostly require a maximization of the brilliance of a neutron beam. As an example the determination of the exact position of hydrogen atoms in protein structures needs a high flux of cold neutrons to illuminate a small protein single crystal of usually less than 1 mm^3 with a well collimated beam. The same holds for an experiment in which the magnetic structure of an ordered ensemble of magnetic nanoparticles, a so called mesocrystal, is being studied. In both cases the samples available are tiny and high brilliance is needed for a successful experiment to deliver highest flux with low divergence in a small beam diameter.

When offering access to neutrons by accelerator driven neutron sources with sufficient neutron flux and brilliance, neutron experiments will become easily accessible in many areas of science beyond the existing large-scale neutron facilities. Individual research from material research to life sciences including cultural heritage can be performed following scientific demand. Operating such a source on the level of a university laboratory would bring the use of neutrons directly to the users and reach out to many scientific fields. New materials can be characterised just in time parallel to their preparation. Moreover, such a source could serve to promote and disseminate neutron research by students through appropriate education and training programs.

2.1. Chemistry and Material Science

The analysis of light elements like hydrogen in materials is of great importance in many areas such as catalysis, high and low temperature materials, energy storage materials or multilayer chemistry. Neutron diffraction is a versatile method to locate hydrogen in the structure of such materials.

For the understanding of chemical reactivity, reaction kinetics and structure dynamics in energy and functional materials complementary studies using neutrons are required. They will help to develop improved structural materials, new lightweight materials, fuel cells and batteries for mobility, energy production, conversion, and storage. New or more efficient processes for material production and energy handling could be developed and improved using various neutron methods.

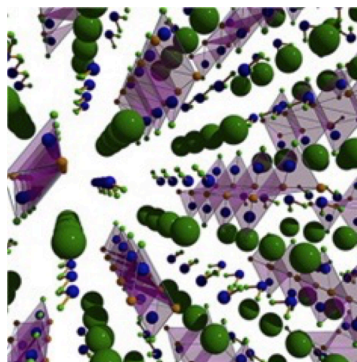


Fig. 2.1. Crystal structure solution of $\text{KMg}(\text{ND})(\text{ND}_2)$: An ordered mixed amide/imide compound [8]

Intermolecular forces in liquids and glasses using high pressure, temperature, or magnetic fields will be studied to understand and improve materials and systems.

Compact accelerator driven neutron sources can be of outmost help in all of these topics using appropriate *diffractometers*, *small angle scattering instruments*, *reflectometers*, *prompt gamma activation analysis* systems or *imaging methods* close to the laboratories and institutes.

2.2. Magnetism and Magnetic Materials

Due to their magnetic moment, neutrons are very prone to study magnetic phenomena ranging from unconventional superconductors and magnetic nanoparticles to magnetic hetero-structures. The magnetic behaviour and structure of novel materials for multiferroics or magneto-calorics can be investigated. Materials for new permanent magnets and applied magnetics materials, of which a high demand in energy, electronics and automotive industry exists, can be developed and tested having easy access to neutrons.

For these and related topics in the field compact accelerator driven neutron sources can provide versatile *neutron diffraction instruments*, *small angle neutron scattering spectrometers*, *reflectometers* and *imaging techniques*. This will allow fast feedback for the exploration of new materials and the neutron methods can be used routinely and complementary to established laboratory studies.

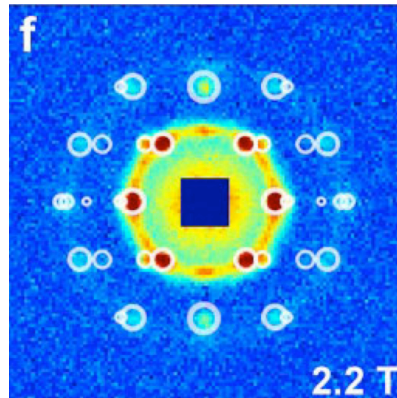


Fig. 2.2. SANS patterns of an iron oxide particle solution [9]

2.3. Engineering

Complex engineering devices can be studied by neutron imaging techniques thanks to the high penetration depth of neutrons in matter. Working systems in real operation conditions can be visualised. Hydrogen containing materials as plastics, oils or soft tissues can be distinguished easily due to the high contrast of hydrogen material in the neutron image as demonstrated on the distribution of oil and lubricants in motor engines improving efficiency and stability of combustion engines.



Fig. 2.3. Studying nickel-based superalloys with neutron diffraction [10]

Steel construction in bridges, lightweight aluminium components in airplanes or cars, rails and axis in trucks or rails have to withstand various kinds of external and internal stress and strain. To monitor such stress and understand the underlying processes and process parameters neutron diffraction is applied providing high spatial resolution and high penetration depth. The analysis of microstructures and phase distribution in composite materials and alloys is important to develop new materials to improve sustainability, save energy and protect environment. Experiments with neutrons will help to verify model predictions and improve material simulation efforts.

In many industrial processes as well as in environmental applications such as water cleaning or energy conversion using fuel cells, porous materials or membranes are needed with dedicated performances. Structure and interaction with gases or fluids can be investigated using small angle neutron scattering, neutron reflectometry or neutron imaging.

Compact accelerator driven neutron sources will offer systematic access to *neutron imaging stations, stress and strain diffractometers, small angle neutron scattering instruments* to enable continuous development for innovation in applied engineering and industry.

2.4. Soft Matter and Biology

Nanocomposites, nanoparticles and nanomaterials for medical and life science are developed and used in an increasing number of applications in daily life, engineering, health care and medicine. Scattering methods to study structure and dynamics of such materials to characterize different formulations and behaviour over time are of general importance. Aspects of safety on health and environment of such new materials have to be studied, which needs reliable structural information. Here, neutron scattering methods can provide important and complementary information. As an example, small angle neutron scattering has been applied to study nanoparticles as drug delivery systems to understand their aggregation and interaction behaviour.

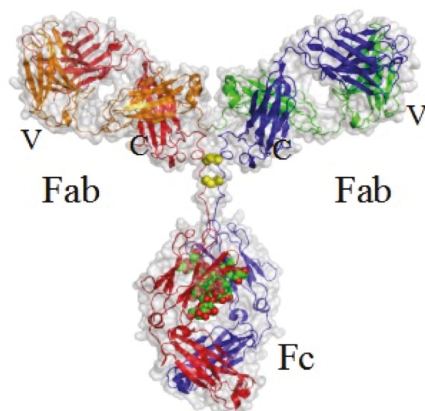


Fig. 2.4. Domain structure of Immunoglobulin IgG1 [11]

New biopolymers and bio-degradable materials are strongly requested for ecologically friendly and energy saving materials and products. Structure and interaction need to be investigated to develop and modify synthesizing processes and adapt to environmental requirements. Deuterated molecules highlight polymer interactions or interaction of drugs and peptides with bio-membranes.

Dedicated instruments on *small angle neutron scattering* and *neutron reflectometry* provided at a compact accelerator driven neutron source will allow systematic studies close to the laboratory in these areas.

2.5 Cultural Heritage

Being a non-destructive probe, neutrons can penetrate deeply into cultural artefacts or beneath the surface of paintings to reveal structures at the microscopic scale, chemical composition, or provide 3D images of the inner parts of the artefacts. For heritage science purposes, whole artefacts can be placed in the neutron beam and analysed at ambient conditions without tedious sample preparation.

Measurements at *neutron imaging stations* are made in real time, which can be useful for testing conservation materials and methods. *Prompt gamma neutron activation analysis* (PGNAA) can be applied for the non-destructive chemical analysis of artefacts.

Often due to the high commercial value of cultural artefacts or objects of art scientific measurements at large scale facilities are extremely difficult, if not even impossible. Compact accelerator driven neutron sources in the vicinity of museums or in the research laboratory of a national museum would enable more studies in this field.



Fig. 2.5. Egyptian statuettes of Osiris: production unveiled by neutrons and laser. [12]

2.6 Education and Training

Before young scientists apply advanced analysis or simulation methods at large scale facilities such as synchrotrons, aberration corrected electron microscopes or supercomputers, they need to be trained in the laboratory scale, at x-ray diffractometers, optical or standard electron microscopes or workstations. However, this option does not yet exist for neutron scattering, where at present corresponding laboratories at universities do not exist. Compact neutron sources can resolve this shortcoming in the future.

Due to the overwhelming pressure at large scale, high power facilities to optimize the use of beam time, they are usually intolerant to trainees. A compact neutron source will offer training possibilities that cannot be entertained at high power sources, ensuring a sustainable high level of competence in neutron science. In particular, at smaller sources, there are much more opportunities for training in the science of neutron production and instrumentation development, in addition to training in the collection and interpretation of data collected on conventional instruments available at major sources.

Beam time to carry out training programs can be allocated specifically, in addition to having students participate in on-going experiments. Furthermore, experimental stations can be envisioned, in modular form, which allow hands on training to take place. In general, this would not be possible at high power sources. Small scale, local or regional neutron sources often have close ties to local universities, so that training programs at the sources can be directly linked to university lecture programs in various domains. Together with specialised instrumentation, this would facilitate the mobility of students and researchers during training and encourage international collaboration.

2.7 Industry, Method development

Low to medium flux neutron sources can well have a high potential for technological applications, dedicated applied research, non-destructive testing and systems development. Fast and easy access to neutrons can help industry to exploit neutrons and use neutron methods to solve specific problems. Dedicated instruments and specialised sample environment for industrial applications could be made available. Industry could participate in the operation of specific instruments or employ own accelerator based neutron sources for their particular requirements. For industry, nondisclosure and immediate access to instruments are key issues, often much more important than higher flux. These requirements can be realised much more easily at a compact accelerator driven neutron source than at one of the few large-scale facilities.

As directions in science change, instrumentation, which enables new measurement possibilities, must be developed. Test beams, or time on instruments, may not be available due to the pressure of carrying out the on-going experimental program. Here, small to medium power sources also have an important role in the development and testing of new instrument concepts and components.

3. Conceptual design of the neutron source

The concept of the neutron source is based on the production of fast neutrons from the interaction of 10 MeV pulsed protons on a water cooled beryllium or vanadium target of appropriate thickness. The initially fast neutrons are slowed down to thermal energy in a moderator and reflector assembly composed of polyethylene and lead, respectively. The choice of the moderator-reflector assembly is driven by the criteria of maximization of the thermal neutron flux and optimization of the time structure of neutron pulses, as well as consideration of cost and manageability. Directed thermal neutron beams are extracted from the location of highest thermal flux inside the moderator through thermal finger beam-lines. Cold neutrons are produced in a cold finger containing a size, temperature, and material optimised liquid (para- or ortho-) hydrogen or solid methane moderator located at the point of maximum thermal neutron flux. Thermal and cold neutrons are extracted using suitable advanced and well tested neutron optics. With this concept, fast, thermal, and cold pulsed neutron beams can be delivered with properties (energy, time structure, divergence, energy resolution) fitting each instrument's requirements. For radioprotection, the moderator and reflector assembly is surrounded by a biological shielding consisting of borated polyethylene and lead.

In this study validated and well established simulation tools were used:

- **SRIM (Stopping and range of ions in mater) [13]:** For the dimensioning of the target thickness according to the target material and proton energy,
- **ANSYS CFX (Computational fluid dynamics) [14]:** For cooling optimization by heat dissipation and for determination of the boundary conditions for ANSYS mechanical calculations,
- **ANSYS, Mechanical [14]:** For target dimensioning and proof of mechanical stability,
- **MCNP6.1. (Monte Carlo N-particle) [15]:** For calculation of the neutron production at the target and the neutron spectra and for the optimization of moderator, reflector and biological shielding.

3.1 Accelerator, Ion Source

For a NOVA ERA type neutron source, a commercially available proton accelerator is needed to produce a pulsed proton beam with particle energy of about 10 MeV. In case of a beryllium target, the energy must be below 13 MeV to avoid tritium production at the target.

Three accelerator types for this energy level are on the market today:

- cyclotrons
- electrostatic accelerators
- RF linear accelerators

RF (Radio Frequency) linear accelerators are the most powerful accelerators available. They can be built up to 100 mA peak current operated at a pulse structure with repetition rate up to several 100 Hz. Due to the high level of engineering of the accelerator structures and the complexity of the RF power supply the price level seems to be too high for a NOVA ERA type

neutron source. If a high-power version of NOVA ERA is desired, a RFI (Rf Focussed Interdigital) linear accelerator would be available up to a peak current of 30 mA [16]. Cyclotrons are typically used for medical applications, i.e. production of radiopharmaceuticals or medical irradiation of patients. For these applications, they produce a CW current of protons or heavier ions with an average current below 2 mA. Such cyclotrons with energy above 18 MeV are commercially available [17]. In principle, the ion source in the centre of the cyclotron can be operated in a pulsed mode, but no company is able to offer a commercial version of a cyclotron based pulsed proton source. Because of that and because of the energy range not exactly matching our requirements, we abandoned this path.

Electrostatic accelerators are typically operated as tandem accelerators, i.e. negatively charged ions (i.e. H^-) are accelerated in an electrostatic field towards a high positive potential (e.g. +5 MV). At the position of the highest potential, where the ions arrive at energy of 5 MeV, the electrons are stripped and positively charged core (i.e. proton, H^+) is again accelerated to ground level, where it arrives with energy of 10 MeV. This kind of accelerator can be equipped with an H^- ion source that delivers more than 1 mA ion current. An electrostatic chopper that is operated between the ion source and the tandem accelerator at an energy level of 50 keV can produce ion pulses with pulse rise and fall time below 50 ns and pulse lengths below 1 ms at every repetition rate desired (see Fig. 3.1). The dimension of such an accelerator with ion source and chopper is shown in Fig. 3.2. The intensity calculations presented in this conceptual design report are based on a tandem accelerator producing a proton beam of 10 MeV energy, 1 mA peak current and 4% duty cycle, i.e. 400 W average ion beam power.

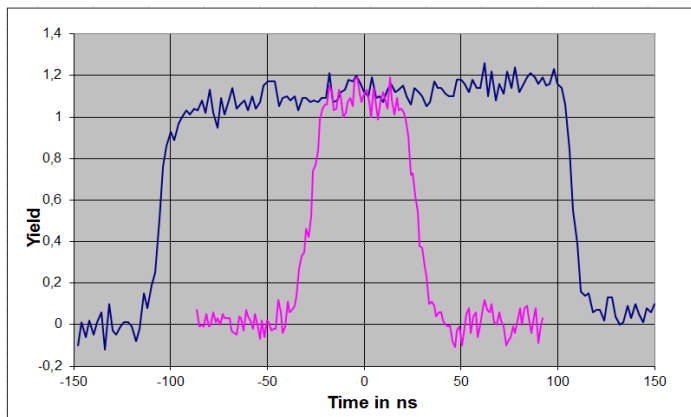


Fig. 3.1. Time distribution of beam intensity resulting from the hard-switched electrostatic chopper (blue line) as offered by High Voltage Engineering B.V. [18]

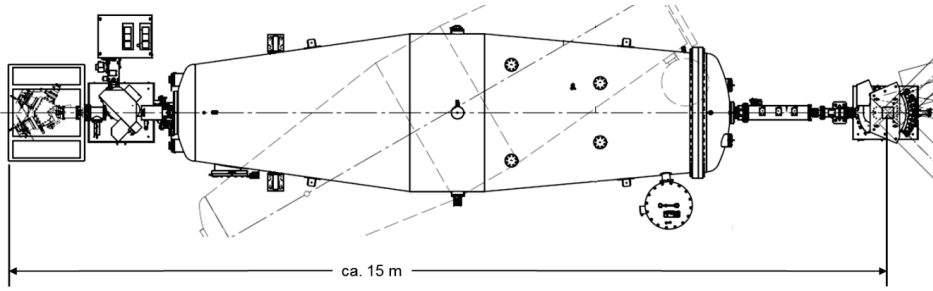


Fig. 3.2. Dimensions of a 5 MV tandem accelerator with ion source, chopper, and switching magnet as offered by High Voltage Engineering B.V. [18]

3.2 Target assembly

Target material

For accelerator based neutron production at low ion energies, beryllium is commonly used as a target material due to a high neutron yield and due to its good mechanical properties. However, beryllium is a strategic and hazardous material and its access might be restricted. Moreover, the European Union has classified beryllium as a critical material. Thus, to overcome a beryllium delivery bottleneck, vanadium which is easy accessible and nontoxic is chosen as an optional target material.

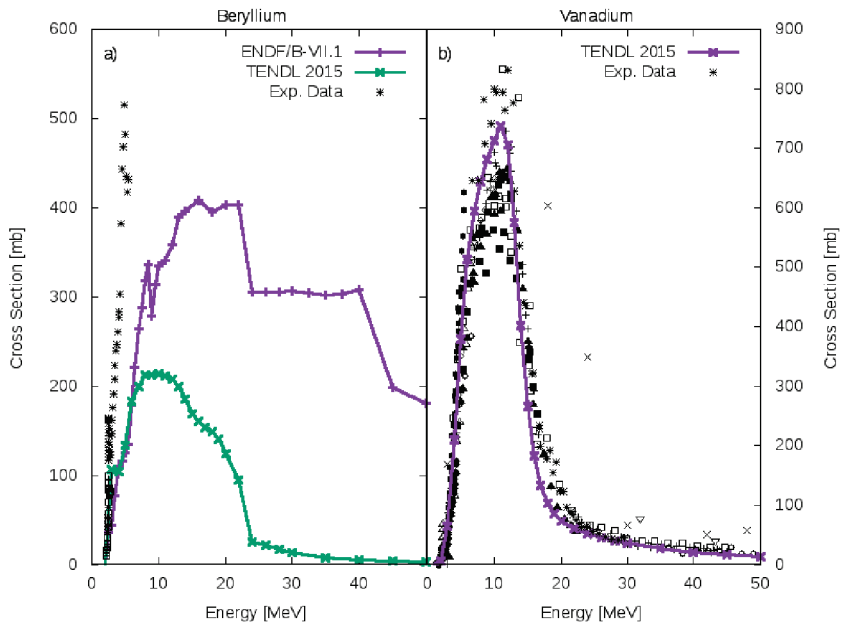


Fig. 3.3. Proton energy dependence of the microscopic cross section for the reactions a) ${}^9\text{Be}(p,n){}^9\text{B}$ and b) ${}^{51}\text{V}(p,n){}^{51}\text{Cr}$. The theoretical data are taken from the ENDF/B-VII.1F [19] and TENDL 2015 [20] databases. The symbols represent experimental data.

Fast neutrons are produced by the nuclear reactions ${}^9\text{Be}(p,n){}^9\text{B}$ and ${}^{51}\text{V}(p,n){}^{51}\text{Cr}$ for a beryllium and a vanadium target, respectively. The proton energy dependence of the microscopic cross sections of these reactions is shown in Fig. 3.3, respectively. For the ${}^9\text{Be}(p,n){}^9\text{B}$ reaction the discrepancies between experimental data (only available up to a proton energy of 5 MeV) and the theoretical data provided by both databases, ENDF/B-VII.1F and TENDL 2015, are very large. Nevertheless, the ENDF/B-VII.1F nuclear database, providing the best estimate of the nuclear cross sections for the ${}^9\text{Be}(p,n){}^9\text{B}$ reaction, is used for numerical simulation. The results of a benchmark for bias estimation from precise experimental data indicate a confidence interval of 54% (2σ) when using this database (Appendix 1). In the case of the ${}^{51}\text{V}(p,n){}^{51}\text{Cr}$ reaction, the cross sections in the TENDL 2015 database agree within $\pm 20\%$ with experimental data. Other proton induced reactions with lower cross sections than the (p,n) reaction but still relevant for radioprotection are shown in Appendix 2. A proton energy of 10 MeV is chosen to remain below the threshold of the ${}^9\text{Be}(p,t){}^7\text{Be}$ reaction at 13 MeV in order to avoid tritium production. The range of protons in beryllium and vanadium is calculated with the SRIM software package. For full stopping of 10 MeV protons a minimum material thickness of 0.8 mm and 0.3 mm, respectively, is required for beryllium and vanadium. To avoid blistering problems due to hydrogen implantation in beryllium [21] a target thickness of 0.7 mm is selected, so that the Bragg peak of the protons, where most of them are fully stopped, lies within the target coolant and not within the Be itself. In the case of vanadium, an element with a very high hydrogen diffusion coefficient ($5 \cdot 10^{-9} \text{ m}^2 \text{ s}^{-1}$ at 25°C [22]), protons can be stopped fully in the target, and therefore the thickness is adjusted to satisfy mechanical stability. For the 0.7 mm thick beryllium target, only 70% of the beam power is deposited in the metal, the remaining 30% being deposited in the cooling water. In the case of vanadium, the full beam power is deposited in the target due to the short range of the protons.

The neutronic properties (total neutron yield, angular distribution, and energy spectrum) are studied by numerical simulations using the MCNP toolkit with the above mentioned nuclear databases. These properties are important for the optimization of the moderator-reflector assembly as well as for the safety aspects related to radioprotection. Primary neutrons' energy spectra and angular distributions induced by 10 MeV protons on beryllium and vanadium are shown in Fig. 3.4. Beryllium and vanadium produce neutron energy spectra of similar shape with a maximum around 1 MeV. The maximum neutron energy is below the reaction threshold of the ${}^9\text{Be}(n,t){}^7\text{Li}$ reaction avoiding the production of tritium. In contrast to vanadium, the beryllium angular distribution is forward directed, thus increasing the neutron density inside the moderator. For beryllium, the estimated neutron yield is $(2.1 \pm 1.1) \cdot 10^{13} \text{ s}^{-1} \text{ mA}^{-1}$ obtained from the analysis of various experimental data [23]. For vanadium, the estimated neutron yield is $(6.7 \pm 1.3) \cdot 10^{12} \text{ s}^{-1} \text{ mA}^{-1}$, i.e. about 1/3 of the Be case.

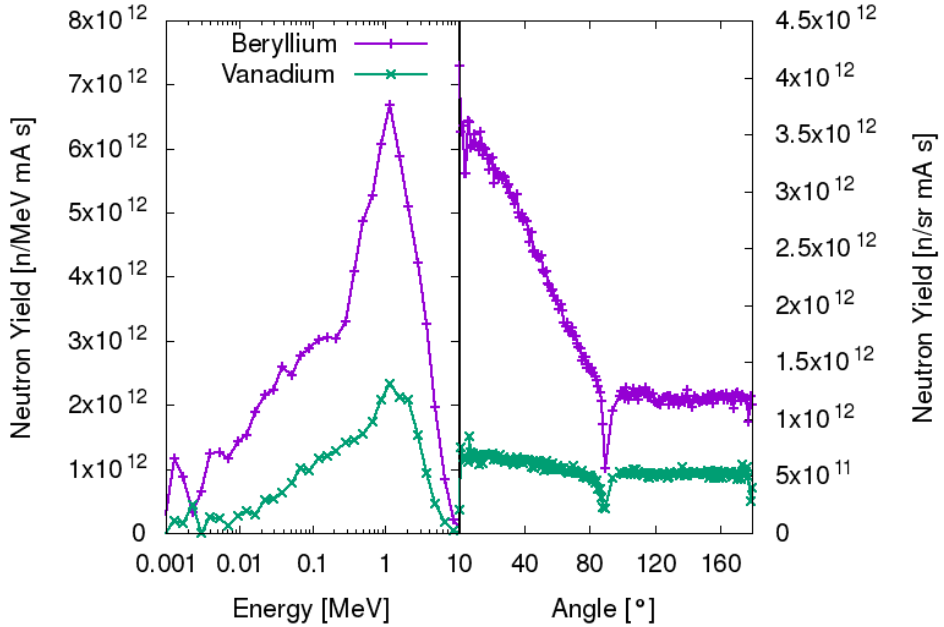


Fig. 3.4. Primary neutrons' energy spectra obtained for the interaction of 10 MeV protons with beryllium and vanadium (left) and corresponding angular distributions for a proton beam of 30 mm diameter (right)

Target design

The target dimension is optimised using the ANSYS CFX toolkit considering the AD2000 guidelines [23] for the beam properties. In the case of the 0.7 mm thick beryllium target, an unsupported circular surface of 40 mm in diameter is the upper limit for mechanical stability and a conservative approximation of 100% (400 W) beam power deposition in the material. For practical reasons, the same unsupported circular surface is used for the vanadium target, while the thickness is set to 1 mm to satisfy mechanical requirements. With the given target geometry and taking into account a safety margin of 5 mm, the proton beam diameter which is variable is fixed to 30 mm. An artistic view of the target assembly with cooling loop embedded in the polyethylene moderator is shown in Fig. 3.5. The target assembly is derived from a reliable system currently in use at the LENS facility adapted to our needs. Its explosion view is shown in Fig. 3.6. It consists of a beryllium or vanadium disc of 80 mm diameter held between two aluminium flanges. Aluminium is a standard construction material with the advantage of low absorption cross section for fast neutrons. Since the target acts as separation between the accelerator vacuum and the cooling water, a reliable and safe sealing is ensured by FKM (Viton) O-rings. To prevent from accelerator damages owing an unexpected fracture of the target the proton beam-line will be equipped with a fast closing shutter.

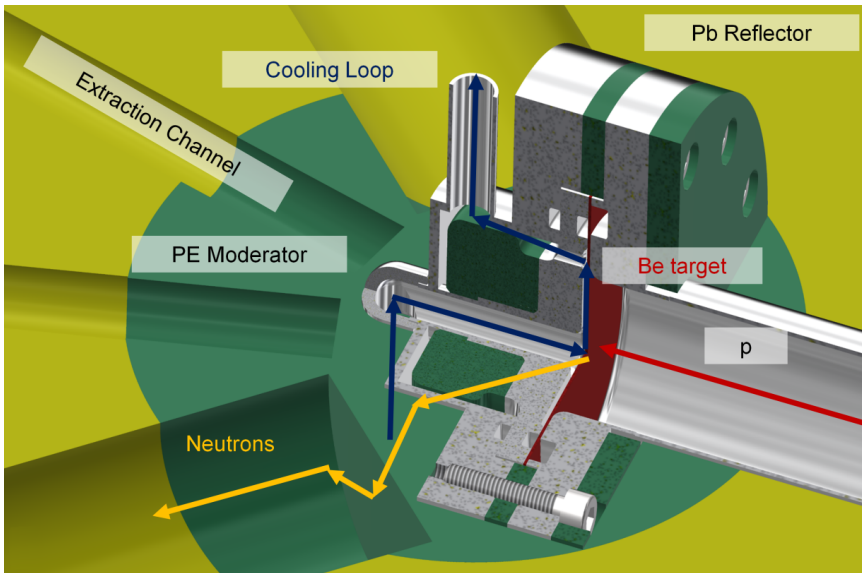


Fig. 3.5. Target assembly with cooling loop embedded in the polyethylene moderator

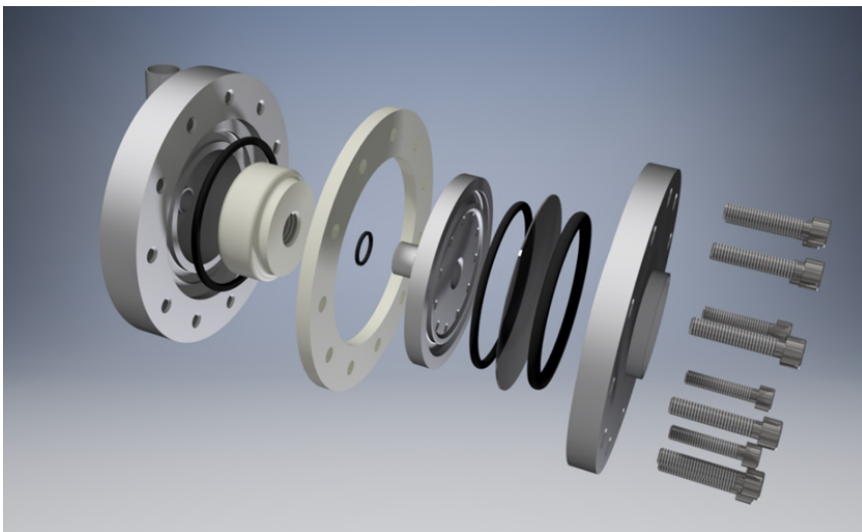


Fig. 3.6. Explosion view showing the components of the target assembly

The cooling system is designed to dissipate the average power of 400 W deposited in the target by using water as coolant. The water hits the target disc at its centre and is forced to spread over the surface through a 1 mm gap. A turbulent flow is induced at the backside of the target disc ensuring a homogenous cooling. Simulations with ANSYS CFX show that a cooling velocity of 3 m/s is sufficient to keep the target temperature below 60°C as shown in Fig. 3.7a. Under this condition, a kinetic pressure of 0.1 bar is not exceeded (see Fig. 3.7b). The mechanical loads due to the kinetic pressure, the pressure difference of 1 bar between

cooling water and accelerator vacuum as well as the thermally induced stress inside the target are investigated using the ANSYS Mechanical tool kit. The boundary conditions were chosen conservatively with a pressure difference between vacuum and cooling water side of 2 bar. Additionally, the 400 W beam power was assumed to be completely deposited within the target material. The mechanical deformation and the von-Mises-stress for the beryllium target under the conditions mentioned above are shown in Fig 3.8. With a maximum deformation of 0.14 mm and a maximum stress of 197 MPa, which is below the yield strength of beryllium, the target can be operated. In the case of vanadium, a target thickness of 1 mm is enough to withstand the loads.

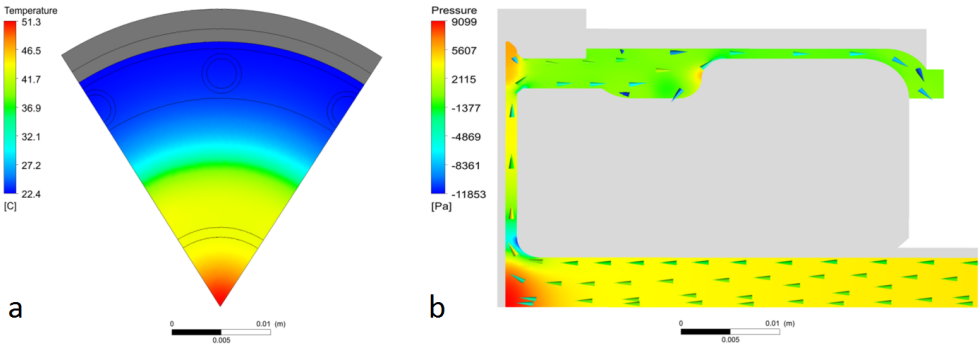


Fig. 3.7. a) Temperature at the beryllium surface on the vacuum side. b) Kinetic pressure component of the water. The arrows indicate the velocity vector of the coolant. For the CFD simulations, a water inlet temperature of 22°C was assumed with an inlet velocity of 3 m/s.

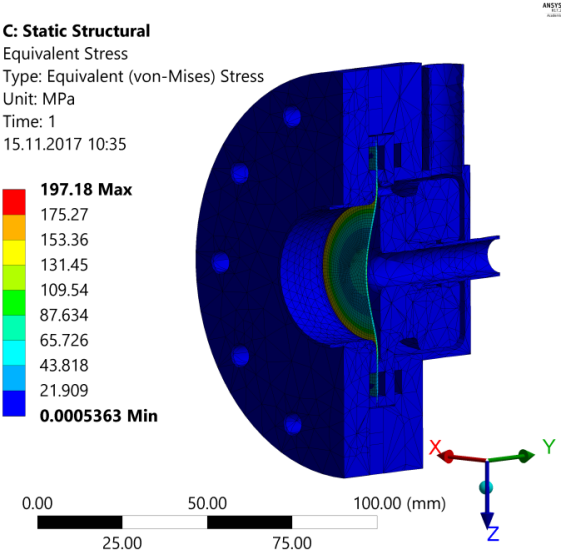


Fig. 3.8. Mechanical deformation and von-Mises-stress for the beryllium target. The colours show the equivalent stress in MPa, while the deformation is visually exaggerated by a factor of 50. The true deformation has a maximum value of 0.14 mm in the centre of the target disc. Local stress maxima are found in the centre of the disc, with values around 140 MPa. At the boundary between the supported and the unsupported area of the beryllium disc the stress is 197 MPa.

3.3 Moderator reflector assembly

MCNP6 simulations have been carried out to determine the dimensions of the moderator-reflector assembly to optimize the thermal neutron flux and time structure of the neutron pulses. A spherical polyethylene moderator is surrounded by a layer of lead for neutron reflection. The geometry of the target and moderator-reflector assembly as used in MCNP6 is shown in Fig. 3.9. The target is positioned at a depth of 5 cm inside the polyethylene moderator.

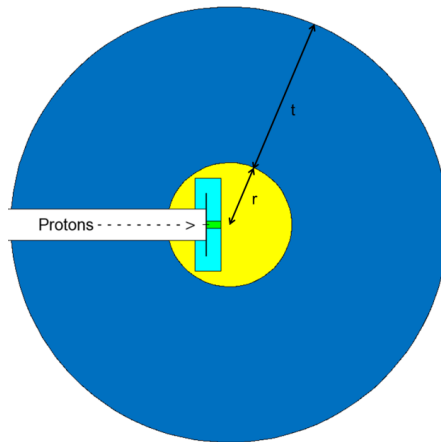


Fig. 3.9. MCNP model of the moderator-reflector assembly including the proton beam-line and the beryllium target. The radius of the polyethylen moderator is r . The thickness of the lead reflector is t . Components displayed are the target (black), the target mounting (cyan), the target coolant (green), the polyethylene moderator (yellow) and the lead reflector (blue). A horizontal cut through the target is shown.

The optimization is performed by varying the moderator radius (r) and reflector thickness (t) using the above mentioned target design with beryllium looking for the maximum value of the thermal neutron flux inside the moderator. The dependence of this value is shown as a function of the moderator radius for various reflector thicknesses in Fig. 3.10. Independently of the reflector thickness a moderator with radius ranging between 8 and 9 cm provides the maximum value. As shown in Fig. 3.10 the reflector thickness may be set to 20 cm; an additional increase of lead providing only a negligible contribution to the maximum value of the thermal flux. Thus, the assembly is composed of an 8 cm radius polyethylene sphere surrounded by a 20 cm lead layer. It may be mentioned that the lead reflector serves also as shielding to attenuate in particularly prompt gamma radiation issues from thermal neutron capture of hydrogen.

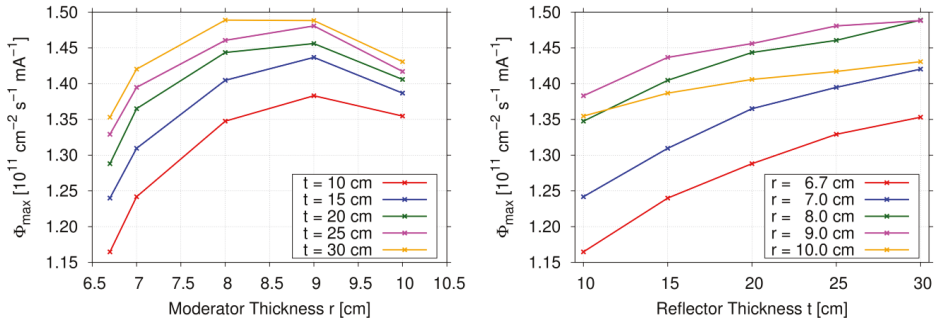


Fig. 3.10. Dependence of the maximum thermal neutron flux on the polyethylene moderator thickness for different thicknesses of the lead reflector (left). Dependence of the maximum thermal neutron flux on the lead reflector thickness for different thicknesses of the polyethylene moderator (right)

The simulated thermal neutron distribution obtained for the beryllium target is shown in Fig. 3.11. The highest thermal neutron flux is observed in the part of the moderator located around 4.5 cm behind the target assembly (in terms of the ion beam direction). For a continuous proton beam of 1 mA its value reaches $1.4 \cdot 10^{11} \text{ cm}^{-2} \text{ s}^{-1}$. For the vanadium target and according to the neutron yields shown in Fig. 3.4 the maximum value of the thermal neutron flux is estimated to be $4.6 \cdot 10^{10} \text{ cm}^{-2} \text{ s}^{-1}$. The time structure of a neutron pulse inside a finite volume at the location of highest neutron flux where the neutrons are extracted is shown in Fig. 3.11. A proton pulse with a flat top of 100 μs has been assumed. The thermal neutron flux is built up during the proton pulse and decreases from the end of the proton pulse exponentially with a die-away time of 210 μs . The full width at half maximum of the neutron pulse is 230 μs . The thermal neutron flux has almost completely vanished after 1.5 ms from the end of the proton pulse.

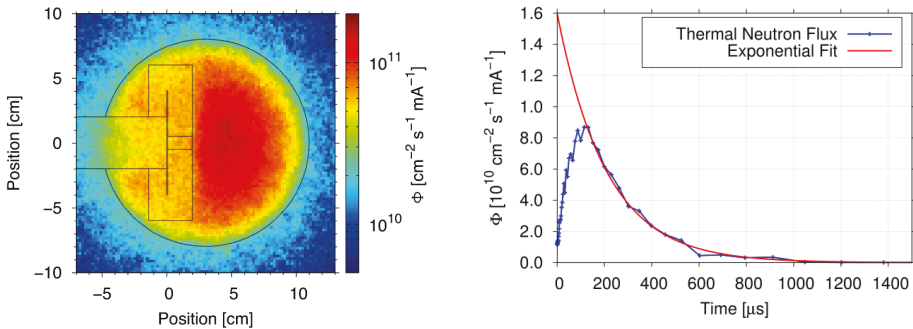


Fig. 3.11. Distribution of the thermal neutron flux inside polyethylene moderator and lead reflector at the middle plane of the beryllium target irradiated with 10 MeV protons (left). Time structure of the thermal neutron flux inside a finite volume at the location of highest neutron flux obtained for a proton pulse of 100 μs (right). The energy range for the thermal neutrons is 13 to 127 meV.

3.4 Source Performance

The source performance such as neutron energy spectrum and total flux, pulse structure and brilliance are calculated at the outer surface of the reflector, exemplarily, for two beam-line configurations using MCNP6. The first configuration, shown in Fig. 3.12a, consists of two channels for thermal neutrons and two channels for cold neutrons. The thermal neutron channels have a diameter of 60 mm and 20 mm, respectively, and are located at angles of -45° and 15° from the proton beam direction. The cold neutron channels have a diameter of 60 mm and 20 mm, respectively, and contain either solid methane (110 cm³ volume, 40 mm long) or parahydrogen (16 cm³ volume, 50 mm long). They are located at angles of 45° and -15° from the proton beam direction. The second configuration is shown at Fig. 3.12b. In contrast to the first configuration the thermal channel with the small diameter is prolonged towards the target to extract fast neutrons.

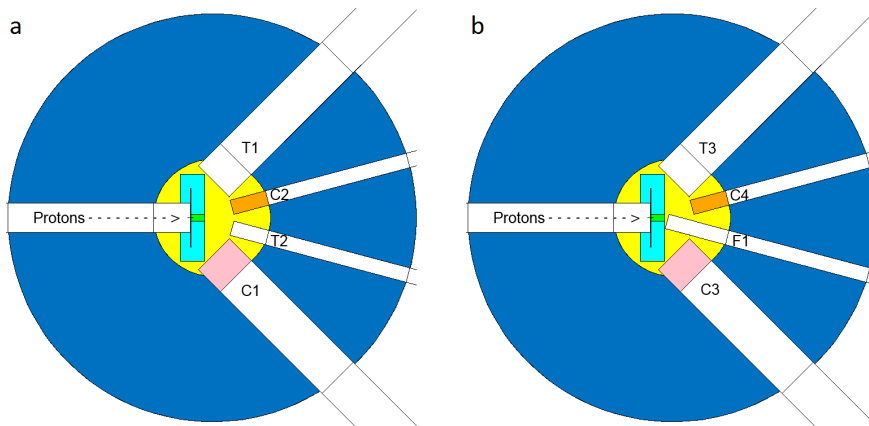


Fig. 3.12. MCNP model of the neutron source. a) Configuration with two channels for thermal neutrons (channels T1 and T2) and two channels for cold neutrons using either solid methane (channel C1) or parahydrogen (channel C2) as cold moderator. b) Configuration with one channel for thermal neutrons (T3), one channel for fast neutrons (F1) and two channels for cold neutrons (channel C3 with solid methane and channel C4 with parahydrogen). Components displayed are the target (black), the target mounting (cyan), the target coolant (green), the polyethylene moderator (yellow), the lead reflector (blue), solid methane (pink) and parahydrogen (orange). A horizontal cut through the target is shown.

The neutron energy spectra obtained for the different neutron channels of the two beam-line configurations are shown in Fig. 3.13 and the resulting values of the cold, thermal, epithermal and fast neutron flux are given in Table 3.1. The presence of the channel F1 for fast neutron extraction instead a thermal neutron channel (T2) does not perturb the cold and thermal neutron fluxes of the cold neutron channels with parahydrogen or solid methane (C1, C3, C2, C4). No perturbation is also observed for the thermal, epithermal and fast neutron fluxes of the thermal neutron channels (T1, T3). The fast neutron channel F1 delivers a fast neutron flux of same order of magnitude than the one of the SR10 fission neutron beam-line at FRM II; however, with a higher contamination by thermal and epithermal neutrons. The latter may easily be filtered using appropriate neutron absorber materials without impacting the fast neutron flux. Due to its position in the polyethylene moderator (see Fig. 3.12), the thermal

neutron channel T2 shows a thermal neutron flux two times higher than the one of the thermal neutron channels T1 or T3, but with a higher fast-to-thermal ratio. For the same reason, the cold neutron channels C2 and C4 with parahydrogen provides higher cold neutron fluxes by a factor 4 compared to the cold neutron channels C1 and C3 with solid methane. However the latter cold neutron channels show a higher cold-to-thermal ratio.

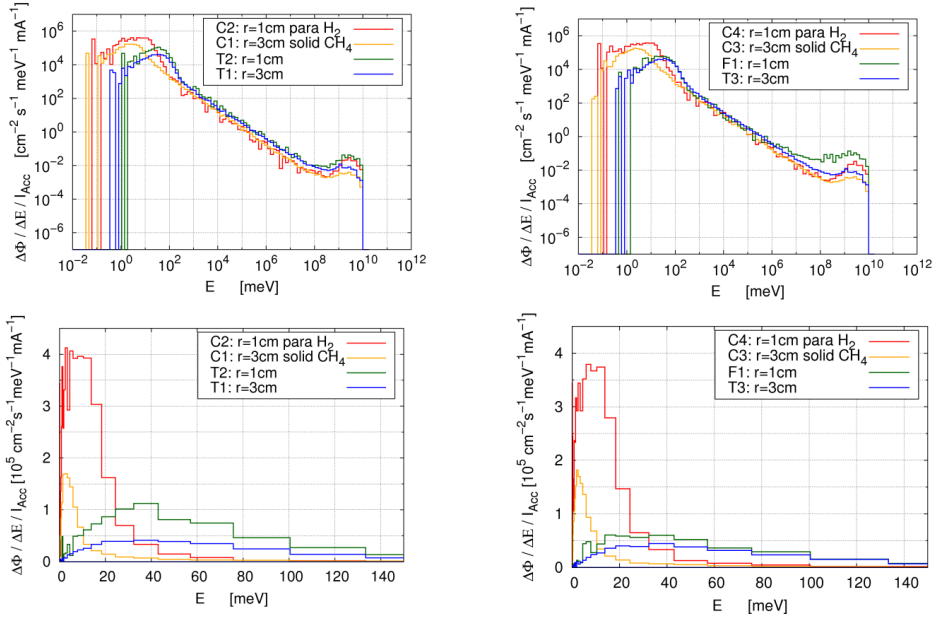


Fig. 3.13. Neutron energy spectra obtained for the neutron channels of the two beam-line configurations shown in figure 3.12. The beryllium target is used for production of fast neutrons.

Table 3.1. Calculated neutrons fluxes ($\text{cm}^{-2} \text{s}^{-1} \text{mA}^{-1}$) in peak at the outer surface of the reflector (forwards direction with an angle of 0.5° with respect to the normal of the surface) for the different channels of the two source configurations described in Fig. 3.12. Energy ranges are: from 0 to 13.1 meV for cold neutrons, from 13.1 to 127 meV for thermal neutrons, from 127 meV to 1 keV for epithermal neutrons and from 1 keV to 10 MeV for fast neutrons. The beryllium target is used for production of fast neutrons. The length of the proton pulse is 100 μs . The uncertainty on the neutron flux values is about 50%.

	Channels of beam-line configuration a				Channels of beam-line configuration b			
	C1	C2	T1	T2	C3	C4	T3	F1
Cold neutrons	$1.12 \cdot 10^6$	$4.28 \cdot 10^6$	-	-	$1.11 \cdot 10^6$	$3.99 \cdot 10^6$	-	-
Thermal neutrons	$4.76 \cdot 10^5$	$3.21 \cdot 10^6$	$2.93 \cdot 10^6$	$6.37 \cdot 10^6$	$4.63 \cdot 10^5$	$3.02 \cdot 10^6$	$2.92 \cdot 10^6$	$3.75 \cdot 10^6$
Epithermal neutrons	-	-	$2.75 \cdot 10^6$	$3.69 \cdot 10^6$	-	-	$2.69 \cdot 10^6$	$2.42 \cdot 10^6$
Fast neutrons	-	-	$4.04 \cdot 10^7$	$2.02 \cdot 10^8$	-	-	$4.03 \cdot 10^7$	$4.85 \cdot 10^8$
Cold/Thermal	2.35	1.33	-	-	2.40	1.32	-	-
Thermal/Epithermal	-	-	1.07	1.73	-	-	1.09	1.55
Fast/Thermal	-	-	13.8	31.7	-	-	13.8	129.3

The time structure of fast, thermal and cold neutron pulses delivered by the thermal neutron channel T2 and the cold neutron channel C2 are shown as an example in Fig. 3.14. The time structures of the neutron pulses obtained for the other channels are given in Appendix 3. Fast neutrons are generated during the length of the proton pulse. After the end of the proton pulse, fast neutrons decay more rapidly in channel C2 than in channel T2 mainly due to the presence of parahydrogen as cold moderator. They completely vanish after 200 μs and 1 ms for channel C2 and T2, respectively, from the beginning of the proton pulse. For the two channels, the thermal neutron flux reaches its maximum value 250 μs after the beginning of the proton pulse and decreases by double exponential decay with die-away-times of 100 μs (short component) and 170 μs (long component). The full width at half maximum of the thermal neutron pulse is 160 μs for the channel T2 and slightly higher, 180 μs , for the channel C2. The cold neutron flux of channel C2 reaches its maximum 350 μs after end of the proton pulse and decreases by double exponential decay with die-away-times of 160 μs (short component) and 300 μs (long component). The full width at half maximum of the cold neutron pulse is 280 μs . Full widths at half maximum and die-away times of the neutron pulses for the other channels are resumed in Appendix 3. The resulting ion pulse length and neutron pulse length after the moderation to thermal and cold energies for typical frequencies with a duty cycle of 4% are given in Table 3.2.

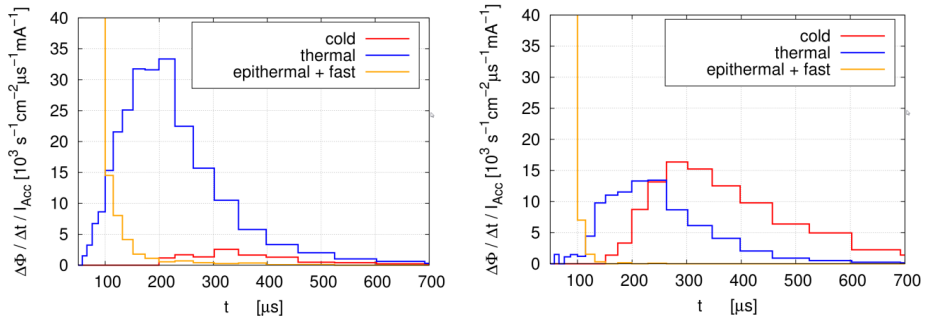


Fig. 3.14. The time structure of fast, thermal and cold neutron pulses delivered by the thermal neutron channel T2 (left) and the cold neutron channel C2 (right) (see Fig. 3.12 for corresponding beam-line configuration). The beryllium target is used for production of fast neutrons. The length of the proton pulse is 100 μs .

Table 3.2. Ion pulse length and neutron pulse length after the moderation to thermal and cold energies for typical repetition rates

Repetition rate (Hz)	Frame length (ms)	Ion pulse length (μs)	Neutron pulse length (μs)	
			Thermal neutrons	Cold neutrons
48	20.8	833	840	870
144	6.9	278	300	380
192	5.2	208	240	330
288	3.5	139	190	290

The brilliance obtained for the thermal and cold neutron channels T2 and C2 is represented in Fig. 3.15. A peak brilliance of about $10^{10} \text{ cm}^{-2}\text{s}^{-1} \text{ sr}^{-1} \text{ \AA}^{-1} \text{ mA}^{-1}$ is achieved for thermal and cold neutrons, respectively. The brilliance for the other channels is shown in Appendix 4. The brilliant beam can be extracted in forward direction up to 2° of divergence with respect to the channel axis. Outside this divergence range, the brilliance is more than one order of magnitude lower. In the case of the cold neutron channel C2, the spectrum outside the central divergence range is thermal.

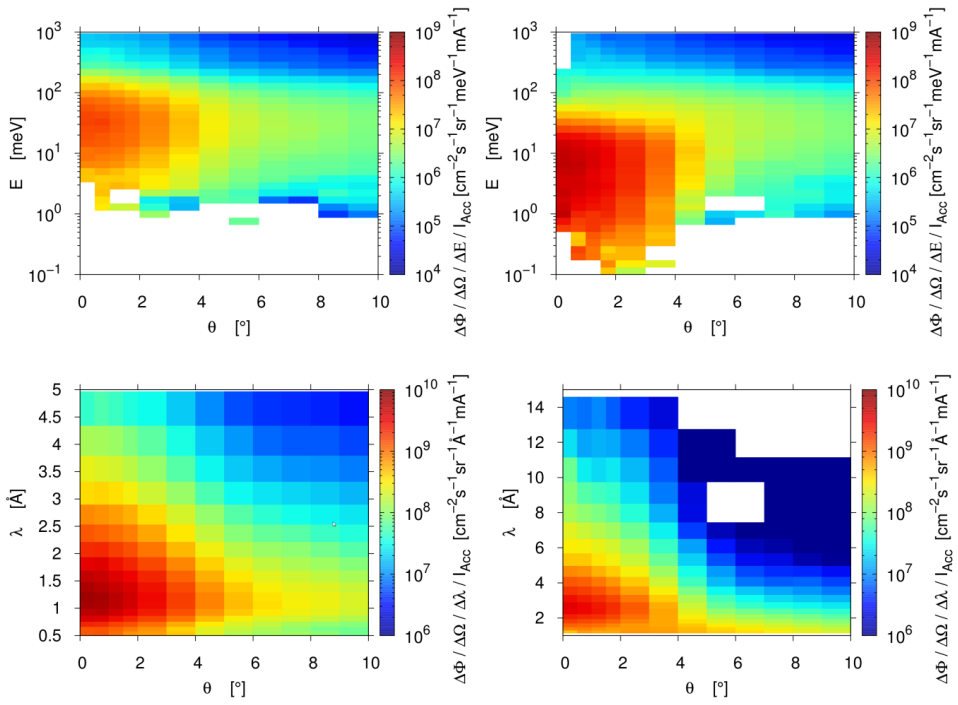


Fig. 3.15. Brilliance delivered by the thermal neutron channel T2 (left) and the cold neutron channel C2 (right) at surface of the lead reflector (see Fig. 3.12 for corresponding beam-line configuration). Note the different wavelength scale for the two cases. The beryllium target is used for the production of fast neutrons.

3.5 Cold moderator

The cold moderator is optimised on the principle of low dimensional moderators proposed for the ESS Butterfly moderator concept [25]. In contrast to the quasi-two dimensional ESS cold moderator, quasi-one dimensional “finger-type” cold moderators are proposed. A small vessel in diameter with a hydrogen rich moderator (methane, ortho-/parahydrogen, or mesitylene) is inserted into the thermal finger and positioned directly at the maximum of the thermal neutron density distribution inside the polyethylene moderator. At this position it is fed from all sides with thermal neutrons moderating them down to cold energies followed by their extraction into beam direction. The geometrical properties should match with the scattering characteristics of the moderator material used.

The optimisation of such cold moderators was conducted by MCNP simulations and the performances were validated experimentally at the AKR-2 reactor of TU Dresden [26]. The liquid hydrogen finger for example is optimised for the use of parahydrogen which has a mean free path of about 1 cm for thermal neutrons and about 10 cm for cold neutrons. Therefore, the vessel has a radius of 1.5 cm and a length of 10 cm, so that thermal neutrons, which try to escape the volume, have a high probability to undergo at least one scattering process, while cold neutrons have a high probability to leave the vessel unhindered. The highest yield of cold neutrons is achieved in forward direction on the outwardly directed surface of the lead reflector (see the figure Fig. 3.15). In the case of solid methane, a more compact cold moderator may be achieved with a vessel of radius of 1.5 cm and of length of about 2.5 cm. Neutron spectra obtained for parahydrogen and solid methane cold moderators of various sizes are shown for total neutron yield in Fig. 3.16. Solid methane delivers a higher cold neutron yield compared to parahydrogen. The maximum yield in parahydrogen is achieved at 8 meV corresponding to 90 K. In the case of solid methane a smooth maximum of the cold neutron flux is observed between 20 K and 80 K. As shown in Fig. 3.16, the brilliance increases by a factor of 2 when approaching low dimensional properties of the moderator by reducing its radius. The gain factor in total number of neutrons useable at the sample position has to be optimised for every instrument taking the dependence of flux and brilliance into account.

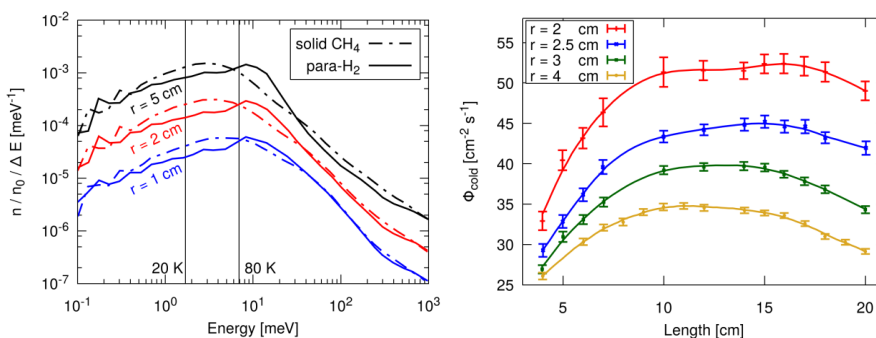


Fig. 3.16. Spectra of neutrons leaving a cylindrical parahydrogen or solid methane cold moderator at 20 K for three different radii (left). The lengths of the cylinders are 4, 5, and 6 cm for parahydrogen and 2, 2.5, and 5 cm for solid methane. The maximum shifts not only with the material, but also with the spin state, since the main low energy scattering mechanism is an induced spin flip. Emitted brilliance at the moderator surface (right). While the total neutron flux is decreasing with the radius (see left diagram), the brilliance is enhanced up to a factor of 2.

The supply of parahydrogen will be generated by a mixing cryostat, in which the spin state from ortho-to-para is changed by catalysis inside a triple heat exchanger providing liquid hydrogen temperatures below 20K (Fig. 3.17).

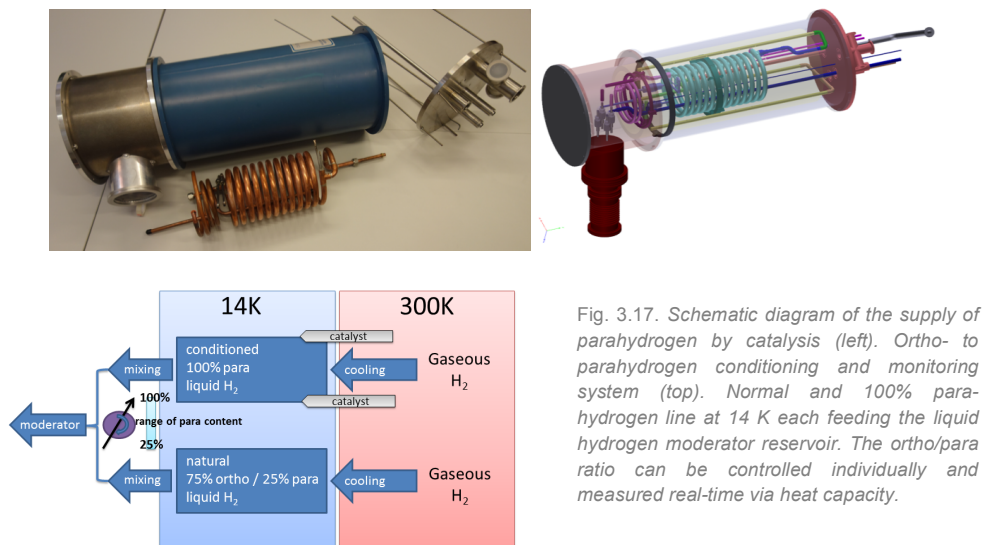


Fig. 3.17. Schematic diagram of the supply of parahydrogen by catalysis (left). Ortho- to parahydrogen conditioning and monitoring system (top). Normal and 100% parahydrogen line at 14 K each feeding the liquid hydrogen moderator reservoir. The ortho/para ratio can be controlled individually and measured real-time via heat capacity.

The cold source prototype developed and built for tests at the AKR-2 is shown in Fig. 3.18. The condensation of hydrogen or methane gas occurs in an aluminium vessel surrounded with a helium gas cooling labyrinth. For liquid hydrogen, the working pressure is defined as 1.5 bar. The cold source is installed on a standard flange and can be inserted into an evacuated beam tube in the thermal polyethylene moderator. Four gas connections are used for input and output of the moderator gas and the helium cooling gas. On the moderator surface towards the beam tube opening, a filter crystal can be mounted for further cleaning of the neutron spectrum. The construction of the finger moderator was performed by ZEA-1 in Jülich [27] and conducted according to DGRL (Druckgeräterichtlinie 97/23/EG with GIP Artikel 3 Abs 3. Since only low pressures and small volumes are used, the safety requirements for the operation of the cold source can be fulfilled with moderate effort according to standard procedures.

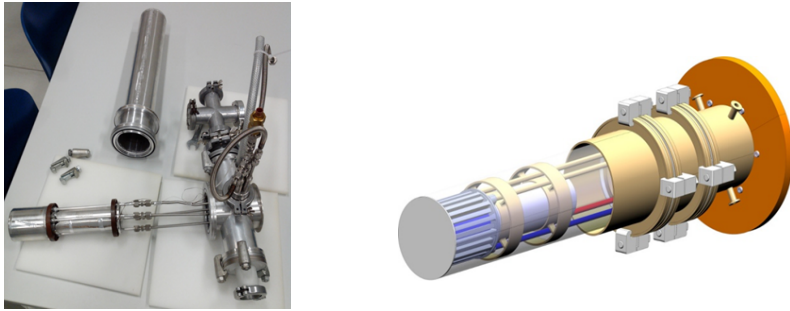


Fig. 3.18. Cold moderator vessel with cryogenic supply and monitoring (left). Technical drawing of the moderator vessel (left). The total length of the vessel is 600 mm.

A safety concept was formulated and approved by the GRS (Gesellschaft für Anlagen- und Reaktorsicherheit) for handling a cryogenic hydrogen, methane or mesitylene moderator within a nuclear facility operating under German Atomic Law (AtG). Since accelerator based neutron sources refer to the German Radiation Protection Ordinance (StrlSchV) safety issues are less pronounced and the approved safety concept can be adapted. The cryogenics needs a supply of liquid nitrogen and liquid helium for cooling and gaseous methane or hydrogen or liquid mesitylene at room temperature if such moderators are chosen. For a university source, cooling agents could be supplied externally, which is customary standard procedure at many universities. For industry, a closed cycle cryostat system can be used, which is nearly maintenance free and easy to operate.

3.6 Biological shielding

The goal of the biological shielding is to maintain the gamma and neutron dose rates as low as reasonably achievable (ALARA principle) to avoid unnecessary radiation exposure of persons working in the adjacent experimental hall during neutron source operation. On the other hand, the biological shielding should be optimised to position the different instruments as close as possible to the neutron source in order to use the neutrons produced more efficiently. The specification of the dose rate limits is set in compliance with the German Radiation Protection Ordinance (StrlSchV) and the minimization requirement. Therefore, the upper dose rate limit chosen is set to 10 mSv/a at the surface of the biological shielding during operation. This value is only half of the dose rate limit for controlled areas according to StrlSchV and hence provides an additional safety margin (conservative approach). The dose rate limit for a supervised area is up to 6 mSv/a according to the StrlSchV. The biological shielding consists of two layers of different materials. The first one surrounds the lead reflector and is made of borated polyethylene (16.1 wt.% B_2O_3), which acts as a fast neutron moderator (polyethylene) and thermal neutron absorber (boron). The second layer is made of lead to reduce gamma radiation which is mainly prompt and issued from thermal neutron capture on hydrogen and boron. The optimization of the thickness of each layer with regards to gamma/neutron dose rate is performed by MCNP6 (ENDF/B-VII.1 database) using a simplified model of the neutron source. In this model shown in Fig. 3.19 the beryllium target without assembly is used (compared to vanadium beryllium shows the highest neutron emission) and the neutron channels depicted in Fig. 3.12 are not implemented. The gamma and neutron dose rates are determined for point detectors positioned forward and backward

on the axis of the proton beam as depicted in Fig. 3.18 as well as averaged over the surface of the biological shielding. The point detectors are directly behind the surface of the shielding. Preliminary studies show that a thickness of 10 cm lead is sufficient to reduce the average surface gamma dose rate below 5 mSv/a. Results concerning the optimization of the thickness of the borated polyethylene layer are shown in Table 3.3. The dose rates correspond to a pulsed source with a neutron emission of $2.1 \cdot 10^{13} \text{ s}^{-1} \text{ mA}^{-1}$ operated 2,000 hours without interruption in a year with a duty cycle of 4%.

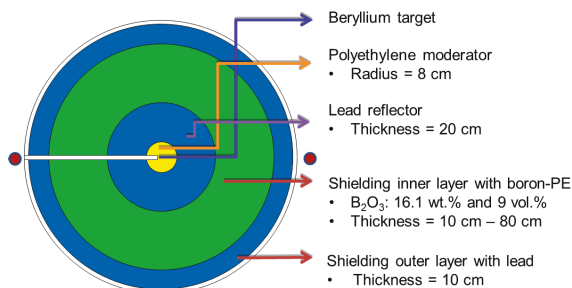


Fig. 3.19. Simplified model of the neutron source for calculation of neutron and gamma dose rates using MCNP 6. A horizontal cut through the target is shown. The proportions of the moderator reflector assembly and the components of the biological shielding are not respected for better visualization. The red surfaces represent the point detectors.

Table 3.3. Neutron and gamma dose rates (DR) at the surface of the biological shielding (average surface flux detector) and at forward and backward point detectors (see. Fig. 3.18) obtained for various thickness of borated polyethylene with 10 cm lead. Pulsed source with a neutron emission of $2.1 \cdot 10^{13} \text{ s}^{-1} \text{ mA}^{-1}$ and a duty cycle of 4%.

Thickness of borated PE (cm)	average surface flux detector		forward point detector		backward point detector	
	Neutron DR (mSv/a)	Gamma DR (mSv/a)	Neutron DR (mSv/a)	Gamma DR (mSv/a)	Neutron DR (mSv/a)	Gamma DR (mSv/a)
10	65	0.2	293	0.06	25	75
20	36	0.04	24	0.008	15	47
30	5	0.02	3.5	0.02	10	36
40	0.8	0.004	0.3	0.002	7.6	25
50	0.3	0.004	0.04	0.0008	5.8	19.6
60	0.2	0.002	0.002	0.001	4.6	16.4
70	0.1	0.001	0.0003	0.0003	4.0	13.7
80	0.03	0.0004	0.00004	0.0003	3.1	10.5

The results show that a shielding made of 30 cm borated polyethylene lined with 10 cm lead is effective and sufficient in order to satisfy the dose criterion set. Neutron and gamma dose rate distributions obtained for this shielding configuration are shown in Fig. 3.20. A large contribution of the dose rate across the outer surface comes from the backward point detector location. This detector is located directly behind the target beam-line without any shielding material in between. The radiation coming through this gap will necessitate an additional shielding on the accelerator side.

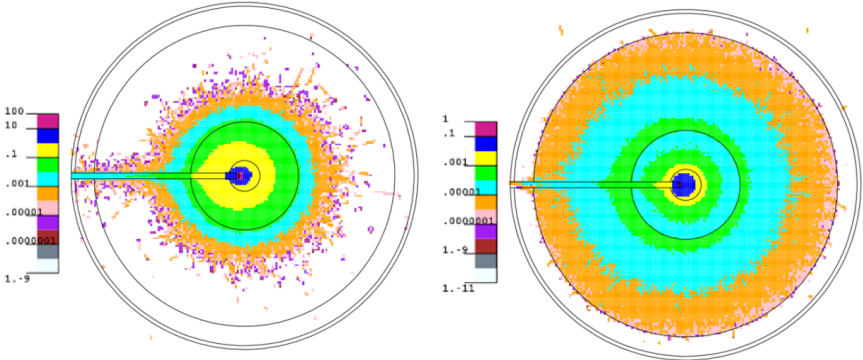


Fig. 3.20. Neutron (left) and gamma (right) dose rate distributions calculated by using MCNP6 for a shielding made of 30 cm borated polyethylene surrounded with 10 cm lead. The unit of the colour legend is 10 mSv/h/source-particle.

4. Instruments

The instrumentation to be installed at a NOVA ERA neutron source strongly depends on the character of investigations that shall be performed. In this chapter, we present a suite of instruments which may be operated at NOVA ERA. Typically, not all of them will be installed, but the owner institution of the installation will choose some instruments matching their scientific demands.

The instruments presented cover the fields of chemical analysis, imaging, and elastic neutron scattering. In general, inelastic neutron scattering instruments will need a stronger neutron source than NOVA ERA. The instruments presented here do not reach the level of the instrumentation at a medium-flux research reactor, but they offer a reasonable level of scientific or engineering investigations close to a laboratory facility without the need to apply and wait for beam time at an external facility.

4.1 Prompt and Delayed Gamma Neutron Activation Analysis

Prompt Gamma Neutron Activation Analysis (PGNAA) using cold or thermal neutron beams is a powerful non-destructive analytical technique to determine the elemental or isotopic composition of small samples of various origins (geological, environmental, biological, pharmaceutical, cultural and industrial). It is based on the measurement of prompt gamma rays emitted during the de-excitation of compound nuclei formed from neutron capture in the sample.

Prompt gamma rays are detected with a collimated HPGe detector (high purity germanium detector) which is cooled electrically or with liquid nitrogen. For Compton background reduction, i.e. improvement of counting statistics, the HPGe detector is surrounded by a guard detector (BGO – Bismuth Germanium Oxide scintillator). The detection system is shielded against gamma background using lead or tungsten and against neutrons scattered from the samples with ${}^6\text{Li}$ containing materials. The sample is placed in a well shielded irradiation chamber which inner surface is lined with ${}^6\text{Li}$ containing materials to absorb scattered neutrons. This reduces the environmental background and avoids material activation. Besides conventional PGNAA of small samples, the pulsed neutron source NOVA ERA will allow to perform prompt and delayed gamma neutron activation analysis with neutron time-of-flight (TOF-P&DGNAA) in order to determine the elemental composition of heterogeneous large samples (Fig. 4.1). This analytical method is based on the measurement of prompt gamma radiation induced by neutron groups of various energies having different sample penetration depths and therefore interrogating different sample volumes. An under-moderated parahydrogen cold source (Channel C2 or C4, Fig. 3.12) is used here to provide an optimal thermal and epithermal neutron flux at the sample position. Cold neutrons are guided to the sample using an elliptic guide equipped with an $m = 4$ supermirror. Neutrons with energies lower than about 4 meV are rejected using a bandwidth mirror positioned at the half length of the neutron guide. A beam size changer allows investigating small or large samples as well. The distance of 10 m between sample and neutron source allows the time-resolved acquisition of prompt gamma-ray spectra at various neutron energies ranging between 4 meV and 30 keV. The peak neutron fluxes estimated for various neutron energy ranges for a neutron pulse length of 870 μs given in Table 3.4. The

average neutron flux at the sample position is about $5 \cdot 10^5 \text{ cm}^{-2} \text{ s}^{-1}$. The integral neutron flux (in peak) over the energy range 4.3 to 115 meV is $1.4 \cdot 10^7 \text{ cm}^{-2} \text{ s}^{-1}$. It is of same order than the equivalent thermal neutron flux of the PGNA station at the TRIGA MARK II reactor of the Oregon State University, $3 \cdot 10^7 \text{ cm}^{-2} \text{ s}^{-1}$ [28]

Additional information for the quantification is provided by neutron detectors measuring the sample neutron transmission as well as local neutron scattering properties of the sample. The neutron energy band is limited towards low energies by a bandwidth mirror, so that the supply of neutrons vanishes within the timeframe of one pulse. Before the start of next fast neutron pulse, delayed gamma rays from activation products with a longer lifetime than the frame length can be measured.

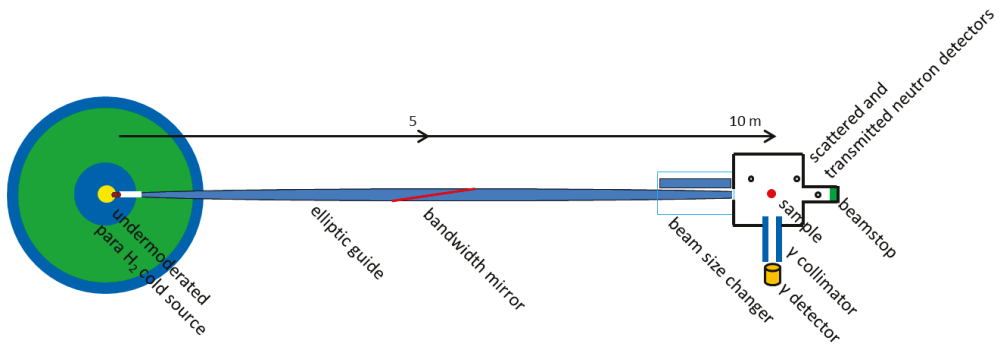


Fig. 4.1. Schematic view of the neutron source NOVA ERA with the instrument for prompt and delayed gamma neutron activation analysis with neutron time-of-flight (TOF-P&DGNA)

Table 4.1. Estimated neutron fluxes (in peak) for various neutron energy ranges and for a neutron pulse length of 870 μs (48 Hz frequency, 4% duty cycle).

TOF range (ms)	Energy range (meV)	Neutron flux ($\text{cm}^{-2} \text{ s}^{-1}$)	TOF range (ms)	Energy range (meV)	Neutron flux ($\text{cm}^{-2} \text{ s}^{-1}$)
11 – 10.5	4.3 – 5.7	$9.7 \cdot 10^5$	6.0 – 5.5	15 – 24	$5.0 \cdot 10^5$
10.5 – 10	4.8 – 6.1	$1.4 \cdot 10^6$	5.5 – 5.0	17 – 31	$3.5 \cdot 10^5$
10 – 9.5	5.1 – 7.0	$1.3 \cdot 10^6$	5.0 – 4.5	21 – 40	$1.6 \cdot 10^5$
9.5 – 9.0	5.8 – 7.9	$1.8 \cdot 10^6$	4.5 – 4.0	26 – 54	$8.0 \cdot 10^4$
9.0 – 8.5	6.5 – 9.0	$2.1 \cdot 10^6$	4.0 – 3.5	32 – 76	$3.2 \cdot 10^4$
8.5 – 8.0	7 – 10.5	$1.7 \cdot 10^6$	3.5 – 3.0	43 – 115	$1.1 \cdot 10^4$
8.0 – 7.5	8 – 12	$1.3 \cdot 10^6$	3.0 – 2.5	58 – 193	$6.6 \cdot 10^3$
7.5 – 7.0	9 – 14	$1.2 \cdot 10^6$	2.5 – 2.0	84 – 410	$3.4 \cdot 10^3$
7.0 – 6.5	11 – 17	$8.2 \cdot 10^5$	2.0 – 1.5	131 – 1319	$6.4 \cdot 10^3$
6.5 – 6.0	12 – 20	$4.4 \cdot 10^5$	1.5 – 1.0	233 – 30394	$5.4 \cdot 10^3$

4.2 Neutron Imaging

Neutron Imaging (radiography/tomography) is widely used in research, industry or medical fields to investigate the internal structure of materials or to study dynamical processes. It is based on the measurement of the neutron attenuation properties of an object using, for example, a CCD camera or a flat-panel silicon detector, after conversion of the neutron energy into light with an appropriate scintillator. Depending on the sample thickness and/or composition, neutron imaging is performed with cold, thermal or fast neutrons. Fast neutron imaging (Fig. 4.2) and cold/thermal neutron imaging with neutron time-of-flight – energy dispersive imaging – (Fig. 4.3) can be performed with the pulsed neutron source NOVA ERA. The fast neutrons are extracted close to the target (Channel F1, Fig. 3.12) and collimated to deliver a beam with a cross section of $40 \times 40 \text{ cm}^2$ at sample position. The thermal and epithermal neutrons are absorbed using a boron or cadmium filter placed in the beam at the height of the lead shielding. The average fast neutron flux at the sample position is $4 \cdot 10^4 \text{ cm}^{-2} \text{ s}^{-1}$. Fast neutrons are detected e.g. with a $41 \times 41 \text{ cm}^2$ amorphous silicon photodiode flat-panel detector linked to an array of scintillating fibres. With a pinhole diameter of 2 cm, a pinhole-to-sample distance of 3 m and a distance between sample and detector of 10 cm, a geometrical resolution of 0.6 mm may be achieved.

Optionally, prompt gamma rays induced by fast neutron inelastic scattering may be measured during imaging to obtain further information on the sample composition. The fast neutron imaging beam-line does not profit from the pulsed operation of the neutron source. Only the detector gate can be disabled between the fast neutron pulses to reduce the background of thermal neutrons that have been moderated in the shielding materials around the sample.

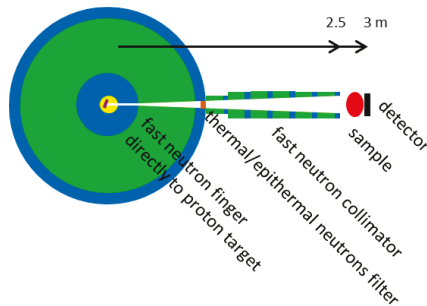


Fig. 4.2. Schematic view of the neutron source NOVA ERA with the instrument for in-beam fast neutron imaging

Cold and thermal neutrons are extracted from a parahydrogen cold source (Channel C2 or C4, Fig. 3.12) and guided to the sample with a 5 m long divergent guide. Afterwards a flight tube is set along the neutron flight path which may be evacuated to reduce neutron scattering and absorption and thus to increase the neutron flux at sample position. The neutron beam size is adjusted to the sample size using beam limiters made of movable boron carbide plates. Sample imaging is carried out with a $41 \times 41 \text{ cm}^2$ amorphous silicon photodiode flat-panel detector linked to a $^6\text{LiF/ZnS:Ag}$ scintillator. With an aperture of 3 cm, a distance of 6 m to the sample and a distance between sample and detector of 10 cm, a geometrical resolution of 0.5 mm may be achieved, i.e. roughly one per mille of the field of view. The time resolution of the detector together with the length of the instrument allows one to determine the wavelength with an accuracy of $\Delta \lambda = 0.3 \text{ \AA}$, which is sufficient to resolve Bragg cut-off wavelengths for crystalline structures. This allows distinguishing between the components of compound materials. At 48 Hz repetition rate, the useful wavelength band is $\lambda = 1 - 7 \text{ \AA}$ with an average flux of $2.5 \cdot 10^3 \text{ cm}^{-2} \text{ s}^{-1}$.

Optionally, prompt gamma-rays induced by cold and thermal neutron absorption may be measured during imaging to obtain further information on the sample composition.

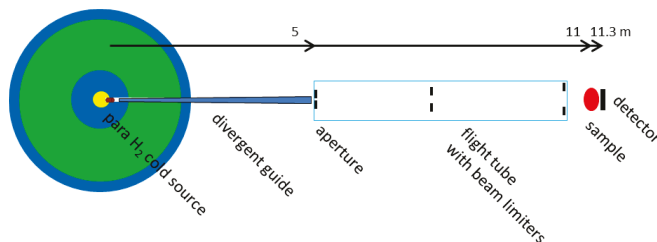


Fig. 4.3. Schematic view of the neutron source NOVA ERA with the instrument for in-beam cold and thermal neutron imaging with time-of-flight resolution of the neutron wavelengths

With the fluxes given above, measurement times of 5 minutes for fast neutron imaging and of around 1 hour for cold/thermal neutron imaging hour one will be sufficient to obtain an image of good quality since a neutron fluence of 10^7 cm^{-2} at sample position is generally required.

4.3 Neutron Reflectometry

A typical pulsed neutron reflectometer is presented in Fig. 4.4. This type of instrument is very well suited to be built at a pulsed source due to the large wavelength band acceptance. As the reflectivity increases strongly with decreasing Q, the drop in spectral density towards long wavelengths is compensated well. A suitable source for a reflectometer is a cold neutron source filled with liquid parahydrogen. We adjust the instrument parameters in such a way that the wavelength band used covers the maximum intensity visible in the phase space maps $\approx 2 \text{ \AA}$ (20 meV) – 10 \AA (0.8 meV). A 10 m long instrument with 48 Hz accelerator frequency will have a wavelength band of 7.5 \AA covering the wavelengths from 2 \AA up to 9.5 \AA selected by a bandwidth chopper in a distance of 5 m from the source. A neutron pulse length of 0.87 ms and an instrument length of 10 m result in a wavelength resolution

of $\Delta\lambda = 0.34 \text{ \AA}$ corresponding to $\Delta\lambda/\lambda = 17\%$ at 2 \AA decreasing to 4% at 9.5 \AA . The neutron guide is curved in the horizontal plane to avoid direct view to the target minimizing the background. A double slit system is mounted directly in front of the sample position with a collimation length of 2 m . The divergence in the horizontal plane can be adjusted with the slit system defining the angular resolution of the reflectometer. In the vertical direction, the slit system is used to reduce the background. In this direction, the reflectometer can accept a large divergence without losing resolution. Therefore, the vertical shape of the guide will be elliptical. In order to transport a sufficient number of neutrons also at short wavelengths, the upper and lower surface of the focusing section of the ellipse will be equipped with $m = 3$ supermirror. For the curved section, the outer side of the neutron guide will be equipped with an $m = 2$ supermirror and the inner part with $m = 1$. In order to estimate the flux at the sample position, we assume a collimation with slits set at $S1 = 10 \text{ mm}$ and $S2 = 10 \text{ mm}$, resulting in a divergence of $\Delta\Theta = 0.3^\circ$ in the horizontal plane. Integrating over the intensity in the phase space maps for the solid angle used and a $\lambda = 2 \text{ \AA} - 9.5 \text{ \AA}$ bandwidth, yields a flux of $5 \cdot 10^4 \text{ cm}^{-2}\text{s}^{-1}$ at the sample position. It is of same order of magnitude as the flux for reflectometry at BER-II (instrument V6), $3 \cdot 10^4 \text{ cm}^{-2}\text{s}^{-1}$ [29].

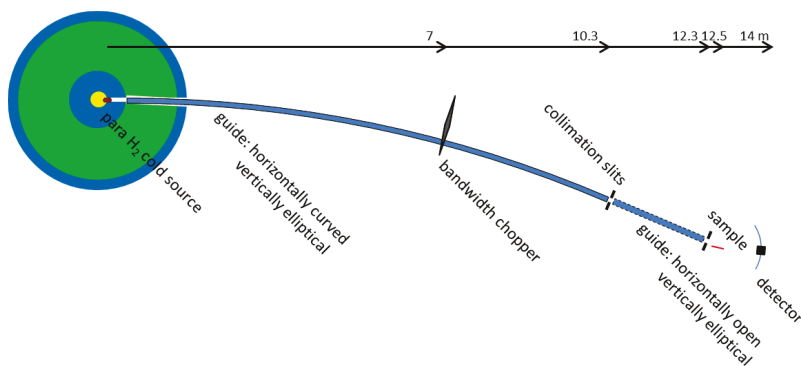


Fig. 4.4. Schematic view of the neutron source NOVA ERA with the instrument for neutron reflectometry

4.4 Small Angle Neutron Scattering

The small angle neutron scattering instrument (SANS), similar to the reflectometer, can use a broad wavelength band and will be built at an extraction channel with a cryogenic moderator. In contrast to the reflectometer, a symmetric divergence, a movable 2-dimensional position sensitive detector and an adjustable collimation length will be employed. The movable detector is necessary to cover the Q-range from low to medium resolution ($3.0 \cdot 10^{-3} \text{ \AA}^{-1}$). The collimation section with neutron guide changer enables one to use a long collimation length for higher resolution experiments as well as a short collimation length for high flux experiments. The total length of the instrument defines the usable wavelength band. Together with the longest collimation and the largest detector distance, we do not want to afford a long curved neutron guide in front of the collimation further reducing the wavelength band. As a compromise for a 30 mm wide neutron guide, we propose the usage of a 2 m long mirror ($m=4$ supermirror) between cold source and the beginning of the collimation to eliminate the direct sight to the target. The SANS instrument proposed is shown in Fig. 4.5.

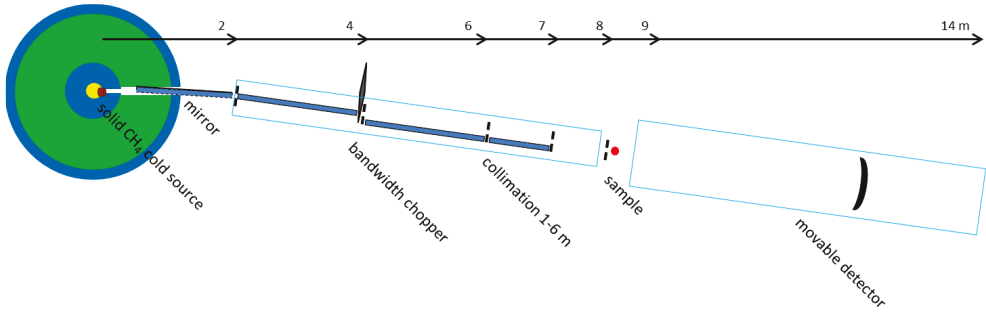


Fig. 4.5. Schematic view of the neutron source NOVA ERA with the instrument for small angle neutron scattering

With different detector distances, different wavelength bands are used and the bandwidth chopper has to be tuned to the requirements of the proposed experiment. Some examples for wavelength band, divergence, slit width and estimated flux at the sample position are presented in Table 4.2. The latter is two to three orders of magnitude lower than the flux at the SANS instrument V4 at BER-II, $2 \cdot 10^7 \text{ cm}^{-2} \text{ s}^{-1}$ [29]. The lower flux can be over-compensated with the easy access to a NOVA ERA type source. A measurement over night at NOVA ERA will have the same scientific outcome as a few hours of beam time at the reactor.

Table 4.2. Estimated flux at the sample position for different collimation lengths and detector distances with resulting wavelength bands for 48 Hz repetition rate and 4% duty cycle

Collimation (m)	Detector (m)	S1 (mm)	S2 (mm)	Divergence (°)	Solid Angle (msr)	λ -band (Å)	Q_{\min} (Å ⁻¹)	Neutron flux (cm ⁻² s ⁻¹)
1	1	20	10	0.86	225	2 – 10.3	$1.8 \cdot 10^{-2}$	$7 \cdot 10^4$
2	2	20	10	0.43	56	2 – 9.5	$1.0 \cdot 10^{-2}$	$2 \cdot 10^4$
4	4	20	10	0.21	14	2 – 8.3	$5.5 \cdot 10^{-3}$	$4 \cdot 10^3$
6	6	20	10	0.14	6.3	2 – 7.4	$4.1 \cdot 10^{-3}$	$1.5 \cdot 10^3$
6	6	10	10	0.10	2.8	2 – 7.4	$3.0 \cdot 10^{-3}$	$6.7 \cdot 10^2$

4.5 Neutron Powder Diffraction

The powder diffractometer presented in Fig. 4.6 differs from the reflectometer and the small angle scattering instrument described above as it is built to resolve atomic structures. This can only be done with thermal neutrons so that the powder diffractometer will be built at a thermal extraction channel. A fast rotating double chopper defines the neutron pulse length and accordingly the wavelength resolution. Between the chopper and the sample position an elliptical neutron guide is used to focus the neutron beam onto the sample. To be able to use a wavelength band as wide as possible, we need to position the double chopper as close to the source as possible to avoid the wavelength dispersion before the pulse passes the chopper. Therefore, the beam-line cannot be shielded against the fast neutron background coming from the source. We need to close the detector acquisition during the ion pulse defining hereby the limits of the natural wavelength band. Changing the frequency of the accelerator pulse structure allows tuning the wavelength band to the experimental requirements.

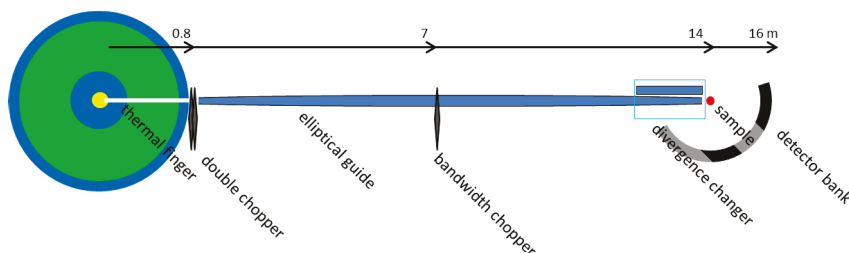


Fig. 4.6. Schematic view of the neutron source NOVA ERA with the instrument for neutron powder diffraction

Table 4.3 shows a selection of useful frequencies, the associated wavelength bands, the resolution and the resulting flux at the sample position for a $25 \mu\text{s}$ neutron pulse length defined by the double chopper. The flux and the resolution scale linearly with the neutron pulse length allowing one to choose the wavelength band freely. For the flux estimate at the sample position, we chose an elliptical neutron guide with $m = 3$ supermirror coating in the focusing section optimised for small samples. With a divergence changer, the focusing section of the neutron guide can be replaced with a straight guide useful to homogeneously illuminate larger samples or for measurements at low Q -values where a small angular divergence is needed. The flux is one order of magnitude lower compared to the powder diffractometer E9 at BER-II, $10^5 \text{ cm}^{-2} \text{ s}^{-1}$ [29].

Table 4.3. Estimated flux at the sample position for different accelerator frequencies and resulting wavelength bands

Frequency (Hz)	λ_{\min} (Å)	λ_{\max} (Å)	$\Delta d/d$ in backscattering	Neutron Flux ($\text{cm}^{-2} \text{s}^{-1}$)
144	1.78	3.42	$2.5 \cdot 10^{-3}$	$2.8 \cdot 10^3$
192	1.34	2.57	$3.2 \cdot 10^{-3}$	$4.3 \cdot 10^3$
192	2.63	3.86	$2.0 \cdot 10^{-3}$	$1.9 \cdot 10^3$
244	0.90	1.73	$5.0 \cdot 10^{-3}$	$5.3 \cdot 10^3$

5. Safety

The German radiation protection ordinance (StrlSchV) forms the legal basis for construction and operation of a facility for production of ionizing radiation (see Appendix 5). According to §11 StrlSchV an official permit including safety requirements is mandatory to operate the neutron source which emits 10^{13} neutrons per second. Furthermore, according to §12 StrlSchV a sufficient number of radiation protection commissioners is required for a safe operation. Requirements for construction and operation of the facility are defined in §13 and §14 StrlSchV, respectively. A general safety concept can be provided; nevertheless, the details must be discussed with the responsible authorities. The operation of the commercial proton accelerator uses for safety proof international standards state of the art techniques, such as beam diagnostic and vacuum control. Furthermore, the neutron channels will be equipped with shutters, the temperature and pressure or mass flow of the target coolant will be monitored continuously, the target temperature and surface from the accelerator side will be monitored continuously by pyrometry and endoscopy. The instrument rooms and the neutron source room will be equipped with safety switches. Moreover, several emergency stop switches will be installed to shut down the accelerator or close the neutron shutters. Neutron and gamma dose rate monitoring systems will be placed in the accelerator room, neutron source room and at the position of the neutron instrumentation.

The proton accelerator will be operated after ensuring that all shutters of the neutron channels are closed and the parameters of the target cooling system are within the limits and accelerator safety switches are activated. The neutron supply for a given experiment is achieved by opening the shutter of the corresponding beam-line according to the regulations of radiation safety. A deactivation of a safety switch at an instrument causes the closing of the shutter of the corresponding beam-line. A deactivation of a safety switch in the neutron room, a deficiency of the target cooling system as well as an increased neutron/gamma local dose rate cause a shutdown of the accelerator. The pyrometry as well as the endoscopy of the target is performed to anticipate a change of the target preventing its fracture and thus a contamination of the proton beam-line and the accelerator. The proton beam tube will in addition be equipped with a fast closing shutter which will prevent from accelerator damages due to an unexpected fracture of the target. All safety measures will be interlocked to accelerator operating.

6. Control Systems

The control systems of NOVA ERA consist of components and tools, which connect all NOVA ERA equipment and present a homogenous and ergonomic interface to operators, engineers and scientists enabling safe and reliable operations. From a control system point of view, NOVA ERA can be subdivided into the neutron source (ion source, accelerator, target, moderator and conventional facilities) and the instruments using these neutrons for research. For NOVA ERA a central control room is foreseen that is permanently manned with operators, whereas instruments are locally controlled by dedicated measurement scripts and programs. Operation of instruments is typically fully automatic, requiring presence of instrument users or scientists only for measurement definition and start, for development and test of dedicated scripts or for sample change. From the perspective of the control system, instruments and source are only loosely coupled via the timing system and the mechanisms to make state information of the machine (e.g. proton charge and energy, omitted pulses) available to the instruments. Due to the loose coupling and the different mode of operation, it is foreseen to have one control system for the machine and individual control systems for each instrument. Since requirements are different, the control systems of the neutron source and the instruments can use different control system technologies and implementation approaches. The neutron source and instrument control systems will be designed as distributed and object oriented systems following the classical three-tier architecture.

6.1 NOVA ERA control system

The NOVA ERA control system can be structured horizontally according to the machine subsystems ion source, accelerator, cooling systems for target and cold moderator, conventional facilities (pressurised air, water, electricity) and the vacuum system for target and cold moderator. Orthogonally to this horizontal structure, the NOVA ERA control system is structured into the following functional groups which are related to all subsystems:

Timing System: Due to the pulse structure of the neutron beam, neutron instruments and NOVA ERA components have to be synchronised. This can be achieved with a central clock that is distributed via a timing network together with event data and trigger pulses. Event receivers have to be implemented at individual devices that decode timing and event data and produce pulses for the synchronization of the device hardware. For neutron detectors a timing resolution below 100 ns is sufficient, but for internal operation of the ion source and beam focusing components of the accelerator, a resolution in the order of 1 ns is envisaged.

Machine Protection System: The Machine Protection System has to avoid machine damage due to device failures or abnormal events like beam loss or failure of a cooling system. The Machine Protection System enforces the safety measures defined in Section 5.

Personal Protection System: The Personal Protection System has to ensure the protection of humans against any hazards from the machine, which may lead to injuries. Main focus is the exposure to radiation, but also other hazards like electrical shock have to be prevented. The personal protection system will be implemented as a highly reliable failsafe system that ensures a safety level according to ISO 13849 PL e (roughly corresponding to IEC 61508 SIL 3). With regard to radiation safety it will manage entrance and exit from radiation

controlled areas. Additionally, radiation levels will be monitored. Any access violation or any violation of radiation level thresholds will lead to immediate shutdown of ion source and accelerator as well as closing of the instrument shutters, as defined in Section 5.

Alarm/Logging System: The alarm and logging system is responsible for collection, distribution and archiving of alarms (information on abnormal situations) and logging events (diagnostic information). A GUI-based console application provides the interface to the operators.

Process Archive: During the operation the HBS machine all relevant process data have to be collected and archived for later analysis.

A special challenge is provided by the fact that the ion source and the accelerator will be delivered by a commercial vendor and it is expected that they will come with their own proprietary control system, whereas control of the other subsystems has to be implemented completely by JCNS. For the integration software, interfaces as well as hardware interlock signals have to be provided by the commercial vendor. Due to the proven competence of Forschungszentrum Jülich in building and maintaining particle accelerators, the required competences for the control system implementation are available. The implementation will be based on control system software tool that is well established in the research community. The most promising and wide spread candidates are EPICS and TANGO, which are both already used in JCNS.

6.2 Instrument control systems

Control of a neutron instrument comprises mainly movement of mechanical axes and access to a wide range of sensors, programmable power supplies and controllers for physical parameters like temperature or pressure. Since event rates and event sizes in neutron detection systems are relatively low compared to nuclear or high energy physics, neutron instruments do not have a dedicated data acquisition system and detector readout is integrated into the instrument control systems. In comparison to the neutron source, the instruments are much more dynamic. They will experience continuous setup changes, especially in the sample environment. There will be a steady change of measurement scenarios, for which dynamic measurement sequences have to be programmed and executed. As a consequence, a more or less static HMI (Human Machine Interface) as required by the NOVA ERA control system is not appropriate for the instrument control system. Instead, the neutron instruments will be controlled by a dedicated instrument measurement program which allows defining, starting and stopping dynamic measurement sequences, typically based on a scripting language.

JCNS has been developing neutron instruments since decades and operates 12 instruments at its main outstation at the MLZ in Garching. All these instruments share the same architecture and technologies for the instrument control systems. In order to minimise the implementation efforts by relying on the existing developments and the support of trained personnel, all NOVA ERA instrument control systems shall be implemented with to the same architecture and the same technologies:

All instrument control systems will be based on TANGO, which has been developed by the ESRF. TANGO is an open-source software toolkit for the development of control systems according to three-tier architecture. MySQL (My Structured Query Language) will be used for all databases (process archives, alarm/logging archives, configuration databases) at the middle tier.

NICOS, developed at MLZ Garching, will be the measurement program for all NOVA ERA instruments. NICOS offers scripting in python and in a simpler command language as well as a configurable GUI (Graphic User Interface) for graphical user operation. Functionalities comprise electronic logbook, history plots and detector data plots. NICOS follows a multiple-client/single-server model, where the server acts as the execution environment for scripts and any device access.

Front-end equipment mainly consists of electromechanical devices like motors, switches, encoders, pumps, valves and different kinds of sensors. Similar to the NOVA ERA control system, all these devices will be controlled by Siemens S7-1500 PLCs with ET200SP and ET200MP decentral periphery systems.

7. Handling of radioactive components

Short, medium and long lived radionuclides are induced by proton and neutron activation of the target and by neutron activation of the target mounting and other components of the neutron source such as moderator, reflector and biological shielding. If these components cannot be reused after an appropriated waiting time they will be disposed as radioactive waste or measured for clearance. The handling of radioactive waste is defined in § 72-79 and clearance procedures in §29 of StrlSchV. According to §72 the yearly amount of radioactive waste produced during the operation time must be estimated.

As an example the activity of the target system is calculated using the elemental composition (including impurities) and the neutron activation fluxes estimated by MCNP given in Table 7.1. The proton induced activity in the target is calculated taking into account the penetration depth (simulated with SRIM) of protons into the material. The activity of radionuclides formed is calculated for two operation scenarios of the neutron source: a 2,000 h operation without interruption (83 days) and a 10 h operation per working day with total operation of 2,000 h (200 days). The activity decay of each radionuclides starting at shut-down of the neutron source is shown for the materials considered and the above mentioned operation scenarios in Appendix 6. The decay of the total activity is shown in Fig. 7.1 for each component.

Activities in the same order of magnitude are obtained for the two operation scenarios. Directly after the shut-down of the neutron source the total activity of the beryllium target is 10^9 Bq and is mainly related to short-lived radionuclide ${}^6\text{He}$ ($T_{1/2} = 808$ ms). After a decay time of about one month, the remaining activity of the beryllium target (10^8 Bq) is mainly caused by the medium-lived radionuclide ${}^{56}\text{Co}$ ($T_{1/2} = 77$ d) which is formed by proton activation of iron impurities in the beryllium target. After one year the total activity (10^6 Bq) is due to the long-lived neutron activation product ${}^{55}\text{Fe}$ ($T_{1/2} = 2.7$ a). In the case of the vanadium target the total activity after shut-down of the neutron source is 10^{11} Bq and is related mainly to ${}^{51}\text{Cr}$ ($T_{1/2} = 27$ d). Up to one year ${}^{51}\text{Cr}$ is still the main radionuclide. Impurities in the vanadium target induce numerous long-lived activation products compared to beryllium target. Furthermore, fast neutron activation of vanadium produces the long-lived radionuclide ${}^{49}\text{V}$ ($T_{1/2} = 330$ d) which activity dominates after one year and cannot be reduced. The total activity of the aluminium mounting is 10^{10} Bq and comes principally from the radionuclides ${}^{24}\text{Na}$ ($T_{1/2} = 15$ h), ${}^{28}\text{Al}$ ($T_{1/2} = 2.2$ min) and ${}^{27}\text{Mg}$ ($T_{1/2} = 9.5$ min). After a decay time of about one month the activity is 10^3 Bq and is mainly due to ${}^{55}\text{Fe}$ ($T_{1/2} = 2.7$ a) induced by interaction of thermal/epithermal and fast neutrons with iron. The total activity of the polyethylene moderator due to the long lived neutron activation products ${}^3\text{H}$ ($T_{1/2} = 12.3$ a), ${}^{14}\text{C}$ ($T_{1/2} = 5,700$ a) and ${}^{10}\text{Be}$ ($T_{1/2} = 1.6 \cdot 10^6$ a) is lower than 1 kBq.

The total activity of the lead reflector after shutdown of the neutron source is 10^9 Bq and is mainly due to the thermal/epithermal neutron activation product ${}^{209}\text{Pb}$ ($T_{1/2} = 3.3$ d). After a decay time of about one year the total activity is about 10^5 Bq and is related mainly to the long-lived activation products ${}^{204}\text{Tl}$ ($T_{1/2} = 3.8$ a) and ${}^{205}\text{Pb}$ ($T_{1/2} = 15.3 \cdot 10^6$ a). The total activity induced in the borated polyethylene as part of the biological shielding may be assumed to be lower than the total activity in the polyethylene moderator due to the presence of boron as a thermal/epithermal neutron absorber. Thermal and epithermal capture of boron produce the radionuclides ${}^{12}\text{B}$ ($T_{1/2} = 20$ ms) and ${}^{10}\text{Be}$ ($T_{1/2} = 1.6 \cdot 10^6$ a) with very low production rates. It may be noticed that one year after shutdown of the neutron source the

activity of the targets and of the lead reflector is of same order of magnitude than the exemption limit given in the StrISchV. In the case of the target mounting, the polyethylene moderator and the borated polyethylene the activities are a factor of about 1,000 lower than the exemption limits.

In order to reduce long term activity, materials with very low impurity content must be used. Furthermore, in the technical design of the neutron source iron should be avoided as structural material and replaced by aluminium.

Table 7.1. Elemental composition of the major used materials used for the design of NOVA ERA and corresponding neutron activation fluxes

	Be-target [30]	V-target [31]	Al-mounting	Pb-reflector	PE-moderator
Element					
H				-	14.3%
Be	99.48%	-	-	-	-
C	1.5 mg/g	-	-	-	86.7%
Mg	0.8 mg/g	1 µg/g	2 µg/g	-	-
Al	1 mg/g	1 µg/g	99.999%	-	-
Si	0.6 mg/g	0.3 mg/g	1 µg/g	-	-
Ca	-	1 µg/g	-	-	-
V	-	99.8%	-	-	-
Cr	-	15 µg/g	-	-	-
Mn	-	1 µg/g	-	-	-
Fe	1.3 mg/g	70 µg/g	1 µg/g	-	-
Cu	-	1 µg/g	1 µg/g	-	-
Ag	-	1 µg/g	-	-	-
Pb	-	-	-	100%	-
Time averaged neutron flux (cm ⁻² s ⁻¹)					
Thermal (E < 120 meV)	7.76 · 10 ¹⁰	2.36 · 10 ¹⁰	7.73 · 10 ¹⁰	3.49 · 10 ⁹	7.01 · 10 ¹⁰
Epithermal (E < 0.5 MeV)	5.56 · 10 ¹¹	2.26 · 10 ¹¹	8.51 · 10 ¹⁰	7.65 · 10 ⁹	6.20 · 10 ¹⁰
Fast (E < 8 MeV)	5.62 · 10 ¹²	1.92 · 10 ¹²	1.52 · 10 ¹¹	4.57 · 10 ⁹	4.50 · 10 ¹⁰

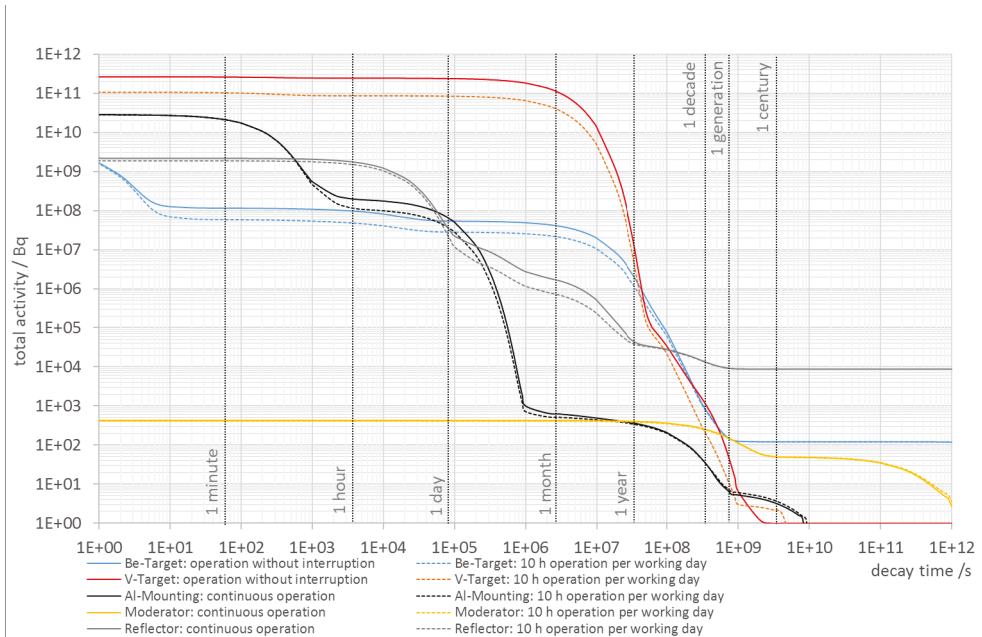


Fig. 7.1. Decay of the total activity induced by irradiation of the beryllium target, the vanadium target and the aluminium mounting for two operation scenarios of the neutron source. Elemental composition of the materials and neutron activation fluxes are given in Table 7.1.

8. Infrastructure

The operation of a NOVA ERA type neutron source is based on a three-zone concept where each zone requires specific infrastructure. The first zone is the accelerator hall containing the tandem accelerator, the ion source, the SF₆ storage tank and the proton beamline with switching magnet. This zone includes also the control room of the neutron source, the high voltage supply and a workshop for accelerator maintenance. For radioprotection, the accelerator hall as supervised area is equipped with neutron and gamma monitoring systems and appropriate shielding. The second zone is the target bunker containing the target station with the closed target cooling circuit, the cryogenic system for the cold moderator (optional) and appropriate devices for maintenance of target station components as well as for target change. According to StrlSchV the target station may be considered as an unsealed source and therefore the target bunker will be defined (probably) as controlled area requiring a ventilation system and air monitoring system. The radioactive components issued from the maintenance of the target station may be stored in an isotope storage room as a part of the target bunker before being released or transferred to a federal state collecting facility. The third zone is the experimental hall containing the neutron guides and the instruments in individual bunkers or with adapted shielding. For radioprotection the experimental hall as supervised area is equipped with neutron and gamma monitoring systems. The area of the individual instruments will be handled as restricted area during operation with open beam. The supply of hydrogen, helium or nitrogen for the cryogenic system is installed outside of the building.

9. Costing

The estimated cost for a NOVA ERA type neutron source (without building structure and instruments) is around 4 Mio. €. The estimated costs for the main components of NOVA ERA are listed in Table 9.1. The cost of the tandem accelerator including ion source, SF6 storage tank, switching magnet and operating system represents about 75% of the total cost. Estimated costs for the target station include the cryogenic system for the cold neutron source(s) (\approx 120 k€), the water cooling system for the target assembly (\approx 110 k€) and the shielding materials (\approx 80 k€). For the other components of the target station such as target, target mounting, moderators, reflector and monitoring instrument costs are ranging between 20 and 40 k€. Estimated costs for safety monitoring instruments include the neutron and gamma monitors, portable contamination and dose rate systems, hand-foot contamination monitor and hydrogen sensors.

Table 9.1. Estimated costs for the main components of a NOVA ERA type neutron source

Position	Estimated costs Mio. €
Accelerator	3.00
Target Station	0.50
Engineering and others	0.20
Monitoring instruments (safety)	0.15
Expertise and approval application	0.10
Sum	\approx 4

The total cost for instrumentation depends on the choice, which instruments shall be installed to cover the scientific or assay needs of the owner institution. In addition, the performance of many instruments can be increased by the installation of a detector system covering a larger angular range. The costs presented here refer to basic detector equipment. The cost for the appropriate neutron optics is included in the costs of the specific instrument.

Table 9.2. Estimated costs for basic NOVA ERA instrumentation

Position	Estimated costs Mio. €
P&DGNAA	0.5
Thermal neutron imaging	0.4
Fast neutron imaging	0.4
Reflectometer	0.7
SANS	1.4
Powder diffractometer	1.5

10. Summary

In the CDR presented here a concept of a compact accelerator driven neutron source called NOVA ERA for science, education and industry is outlined in detail. Technical requirements as well as operational and safety issues are given. A estimate on the costing of such a neutron source is included. Potential performance of instruments to be operated and the scientific impact is described. A comprehensive overview on the main technical and operational parameters is given in the table below.

The NOVA ERA neutron source would bridge the gap between existing large scale neutron facilities and its use as local source at universities and in research institutes as well as industry. Education and training using neutrons would be easily possible and strengthen the impact neutrons can provide for science and innovation.

Table 10.1. Parameters of the NOVA ERA neutron source

Accelerator <ul style="list-style-type: none">- 5 MV electrostatic tandem accelerator- Ions: protons with an end energy of 10 MeV and a current of 1 mA- Variable frequency between 48 and 288 Hz with duty cycle of 4%- Proton pulse length between 139 and 833 μs- Peak power: 10 kW, average power: 400 W
Target <ul style="list-style-type: none">- Beryllium (or Vanadium)- Neutron emission: $\approx 2 \cdot 10^{13} \text{ s}^{-1}$ ($\approx 7 \cdot 10^{12} \text{ s}^{-1}$)- Target cooling: water with a flow rate of 3 m s^{-1}
Moderator/Shielding <ul style="list-style-type: none">- Primary moderator: polyethylene- Cold moderator: para-hydrogen, solid methane, mesitylene- Reflector: 20 cm thick lead- Shielding: 30 cm thick borated polyethylene with 10 cm thick lead- Average surface dose rate: 5 mSv/a (neutron radiation), 0.02 mSv/a (gamma radiation)
Instruments <ul style="list-style-type: none">- Number of neutron channels: 1 to 6- Prompt Gamma and Delayed Gamma Neutron Activation Analysis- Cold/Thermal Neutron Imaging- Fast Neutron Imaging- Neutron Reflectometry- Small Angle Neutron Scattering- Neutron Powder Diffraction

11. References

- [1] ESFRI Scripta Volume I; "Neutron scattering facilities in Europe: present status and future perspectives"; ESFRI Physical Sciences and Engineering Strategy Working Group Neutron Landscape Group; June 2016; Editors: Colin Carlile and Caterina Petrillo
- [2] U. Rücker, T. Cronert, J. Voigt, J. P. Dabruck, P. -E. Doege, J. Ulrich, R. Nabbi, Y. Beßler, M. Butzek, M. Büscher, C. Lange, M. Klaus, T. Gutberlet and T. Brückel; „The Jülich high-brilliance neutron source project"; Eur. Phys. J. Plus, 131 1 (2016) 19; DOI: <http://dx.doi.org/10.1140/epjp/i2016-16019-5>
- [3] G. Mank, G. Bauer, F. Mulhauser; Accelerators for Neutron Generation and Their Application; Rev. Accl. Sci. Tech. 4, 129 (2011)
- [4] <http://www.indiana.edu/~lens/>
- [5] Y. Kiyanagi; JCANS network of compact neutron facilities in Japan; Eur. Phys. J. Plus (2016) 131: 132; <http://dx.doi.org/10.1140/epjp/i2016-16132-5>
- [6] C. Adreani, C.K. Lung, G. Prete; Compact accelerator-driven neutron sources; Eur. Phys. J. Plus (2016)131-217
- [7] J.P. Dabruck, T. Cronert, U. Rücker, Y. Bessler, M. Klaus, C. Lange, M. Butzek, W. Hansen, R. Nabbi, T. Brückel, Development of a moderator system for the High Brilliance Neutron Source project, IL NUOVO CIMENTO 38 C (2015) 192
- [8] E. Napolitano, F. Dolci, R. Campesi, C. Pistidda, M. Hoelzel, P. Moretto, S. Enzo; Crystal structure solution of KMg(ND)(ND₂): An ordered mixed amide/imide compound; Int. J. Hydrogen Energy, 39, 2014, 868-876
- [9] Z. Fu, Y. Xiao, A. Feoktystov, V. Pipich, M.-S. Appavou, Y. Su, E. Feng, W. Jin, T. Brückel; Field-induced self-assembly of iron oxide nanoparticles investigated using small-angle neutron scattering; Nanoscale, 8, (2016), 18541-18550
- [10] www.neutrons.ornl.gov/news/superalloys-under-high-temperature-and-high-stress.html
- [11] L. Stingaciu, O. Ivanova, M. Ohl, R. Biehl, D. Richter, Fast antibody fragment motion: flexible linkers act as entropic spring, Scientific Reports 6, 22148, 2016
- [12] www.nmi3.eu/neutron-research/grand-challenges/heritage-science.html
- [13] J.F. Ziegler, J.P. Biersack, M.D. Ziegler; SRIM – The Stopping and Range of Ions in Matter"; Ion Implantation Press (2008)
- [14] ANSYS Inc., CFX Solver Theory Guide, Release 13, November 2010
- [15] MCNP6 User's Manual Version 1.0, LA-CP-13-00634 Rev. 0, Los Alamos National Laboratory (2013) Pelowitz D. B. (ed.).
- [16] <https://ionlinacs.com>
- [17] <http://www.iba-radiopharmasolutions.com/products/cyclotrons>
- [18] <http://www.highvolteng.com>
- [19] M.B. Chadwick, M. Herman, P. Obložinský, et al., ENDF/B-VII.1 Nuclear Data for Science and Technology: Cross Sections, Covariances, Fission Product Yields and Decay Data, Nuclear Data Sheets, 2887-2996, Volume 112, Issue 12 (2011).
- [20] A.J. Koning and D. Rochman, "Modern Nuclear Data Evaluation with The TALYS Code System", Nuclear Data Sheets 113 (2012) 2841
- [21] T. Rinckel, Target Performance at the Low Energy Neutron Source, Physics Procedia 26 (2012) 168 – 177

- [22] C. Nishimura, M. Komaki, M. Amano, Hydrogen permeation characteristics of vanadium-nickel alloy, *Matter Trans.* (1991), 32(5), 501-507
- [23] W.B. Howard, S.M. Grimes, T.N. Massey, S.I Al-Quraishi, D.K. Jacobs, C.E. Brient, J.C. Yanch, Measurement of the Thick-Target $^9\text{Be}(p,n)$ Neutron Energy Spectra, *Nuclear Science and Engineering*, Issue 2, Volume 138 (2001).
- [24] VdTÜV , AD 2000-Regelwerk, März 2014
- [25] F. Mezei, L. Zanini, A. Takibayev, K. Batkov, E.B. Klinkby, E. Pitcher, T. Schönfeldt, Low dimensional neutron moderators for enhanced source brightness, *Journal of Neutron Research*, Vol 17, (2014) 101-105.
- [26] T. Cronert, J. P. Dabruck, P. E. Doege, Y. Bessler, M. Klaus, M. Hofmann, P. Zakalek, U. Rücker, C. Lange, M. Butzek, W. Hansen, R. Nabbi, T. Brückel, High brilliant thermal and cold moderator for the HBS neutron source project Jülich, VI European Conference on Neutron Scattering (ECNS2015) *Journal of Physics: Conference Series* 746 (2016) 012036
- [27] Bachelorarbeit, Marc Hofmann, Januar 2016, Fachhochschule Aachen, Campus Jülich, Maschinenbau mit Praxissemester, Energietechnik, Nuklearwissenschaften, Auslegung eines kryogenen Flussfingers im Rahmen einer Parameterstudie am AKR-2 als Voruntersuchung zur Entwicklung einer hoch-brillianten Neutronenquelle.
- [28] J.A. Robinson, M. Hartman, S.R. Reese; Design, construction and characterization of a prompt gamma activation analysis facility at the Oregon State University TRIGA® reactor; *J Radioanal Nucl Chem* (2010)283:359-369 M. Tovar, H. A. Graf (Editors), *Neutron Scattering Instrumentation at the Research Reactor BER II*, Berlin Neutron Scattering Center (2007).
- [29] Y. Verzilov, K. Ochiai, M. Yamauchi, A. Klix, M. Wada, T. Nishitani, Impurities in Beryllium, chapter 3.4, Activity report of the Fusion Neutronics Source, JAERI Review 2004-017, 2014
- [30] <http://www.goodfellow.com>, Vanadium Folie, Reinheit 99,8%, Stand 19. Oktober 2017

Appendix 1 Benchmark for neutron emission from a beryllium target

Simulations using Monte Carlo N-Particle transport code MCNP6.1 [15] and ENDF/B-VII.1 data library [19] are performed to estimate neutron emission of beryllium target, to optimize the moderator-reflector assembly and the neutron source shielding. In order to evaluate the uncertainty of the simulation results, a benchmark is carried out by simulating the experimental measurement of the ${}^9\text{Be}(p,n)$ spectrum obtained for 5 MeV protons and described in [23].

The MCNP simulation model of the experimental geometry is shown in Fig. A1.1. The beryllium target is 2.5 cm square and 0.05 cm thick. In order to obtain a good counting statistics according to a reasonable computing time, some simplifications of the experimental arrangement are taken into account. The modelling of the collimator with a diameter of 30 cm in a 1.2 m thick concrete is not implemented and the neutron detector (12.7 cm diameter and 1.27 cm thick) located at 1 meter flight path is replaced by a point detector.



Fig. A1.1. MCNP model of the experimental arrangement described in [23] to measure neutron energy spectra from the ${}^9\text{Be}(p,n)$ reaction

The ratio of the calculated to experimental neutron spectrum is given in Fig. A1.2. For energies below about 0.3 MeV, the calculated and measured values are in good agreement. Between 0.3 MeV to 0.9 MeV as well as above about 1.9 MeV, the calculated neutron fluxes are underestimated. Around 1.0 MeV, the calculated values are almost two times higher than the experimental values.

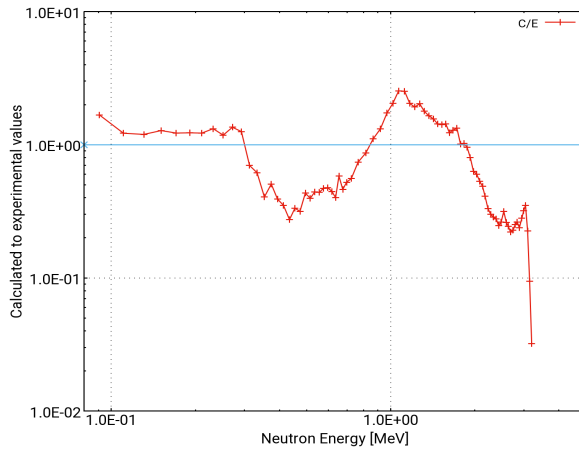


Fig. A1.2. Ratio of calculated to experimental neutron spectrum for the ${}^9\text{Be}(p,n)$ reaction with 5 MeV protons. The bin widths are 20 keV up to neutron energy of 700 keV and are 50 keV otherwise. The energy at the centre of the bins is provided.

The measured zero degree neutron yields obtained in [23] for various proton energies are shown in Fig. A1.3. At 5 MeV proton energy, the fit of the data leads to a neutron yield of $4.43 \cdot 10^8 \text{ sr}^{-1} \mu\text{C}^{-1}$. The total neutron emission calculated by MCNP, $3.24 \cdot 10^8 \text{ sr}^{-1} \mu\text{C}^{-1}$, is underestimated by a factor 1.36. Thus the results of the benchmark indicate a confidence interval of 54% (2σ) when using ENDF/B-VII.1 data library for beryllium.

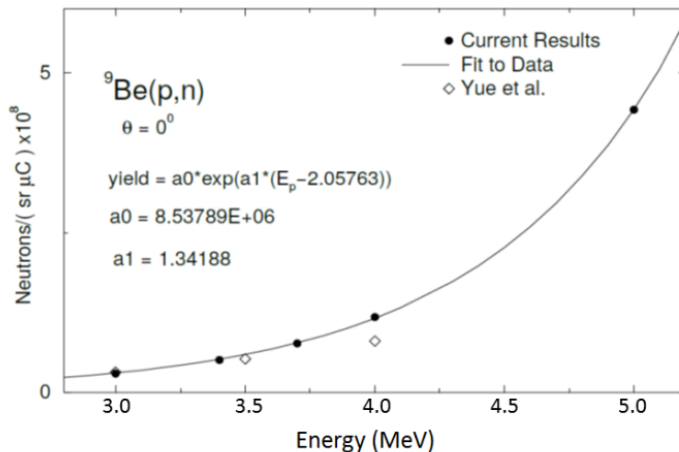


Fig. A1.3. measured zero degree neutron yields at various proton energies [23]

Appendix 2 Proton reactions on beryllium and vanadium with energy thresholds lower than 13 MeV

Reaction	Q-value (MeV)	E-threshold (MeV)
Beryllium		
${}^9\text{Be}(p, \gamma){}^{10}\text{B}$	+6.585	0
${}^9\text{Be}(p, \alpha){}^7\text{Li}$	+2.125	0
${}^9\text{Be}(p, d)\alpha\alpha$	+0.651	0
${}^9\text{Be}(p, d){}^8\text{Be}$	+0.559	0
${}^9\text{Be}(p, pn)\alpha$	-1.573	1.749
${}^9\text{Be}(p, p'n){}^8\text{Be}$	-1.665	1.851
${}^9\text{Be}(p, n){}^9\text{B}$	-1.850	2.057
${}^9\text{Be}(p, \alpha){}^6\text{Li}^* \rightarrow \alpha + n + p$	-2.185	2.312
${}^9\text{Be}(p, p'){}^9\text{Be}^* \rightarrow \alpha + {}^5\text{He}$ ${}^5\text{He} \rightarrow n + \alpha$	-2.46	2.74
${}^9\text{Be}(p, \alpha){}^6\text{Li}^* \rightarrow p + {}^5\text{He}$ ${}^5\text{He} \rightarrow n + \alpha$	-3.245	3.608
${}^9\text{Be}(p, \alpha){}^6\text{Li}^* \rightarrow {}^5\text{Li} + n$	-3.525	3.920
${}^9\text{Be}(p, n\alpha){}^5\text{Li}$	-3.54	3.93
${}^9\text{Be}(p, t){}^7\text{Be}$	-12.081	13.432
${}^{51}\text{V}(p, n){}^{51}\text{Cr}$	-1.534	1.566
${}^{51}\text{V}(p, \gamma){}^{52}\text{Cr}$	10.503	0

Appendix 3 Time structure, full widths at half maximum and die-away times of neutron pulses obtained for the different neutron channels

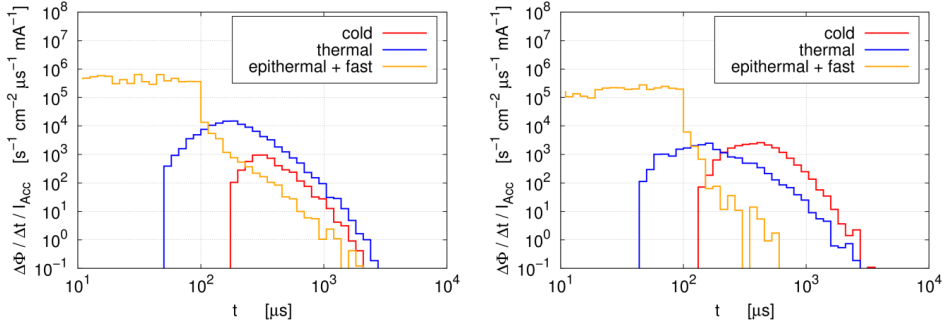


Fig. A3.1. The time structure of fast, thermal and cold neutron pulses delivered by the thermal neutron channel T1 (left) and the cold neutrons channel C1 with solid methane as cold moderator (right) (see Fig. 3.12 for corresponding beam-line configuration). The beryllium target is used for production of fast neutrons. The length of the proton pulse is 100 μs .

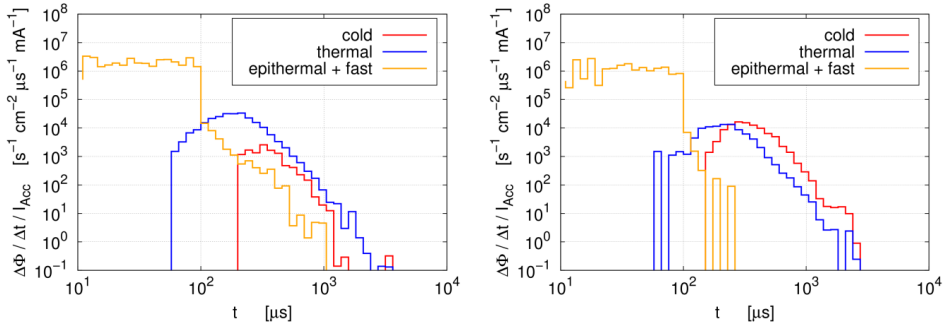


Fig. A3.2. The time structure of fast, thermal and cold neutron pulses delivered by the thermal neutron channel T2 (left) and the cold neutrons channel C2 with liquid parahydrogen as cold moderator (right) (see Fig. 3.12 for corresponding beam-line configuration). The beryllium target is used for production of fast neutrons. The length of the proton pulse is 100 μs .

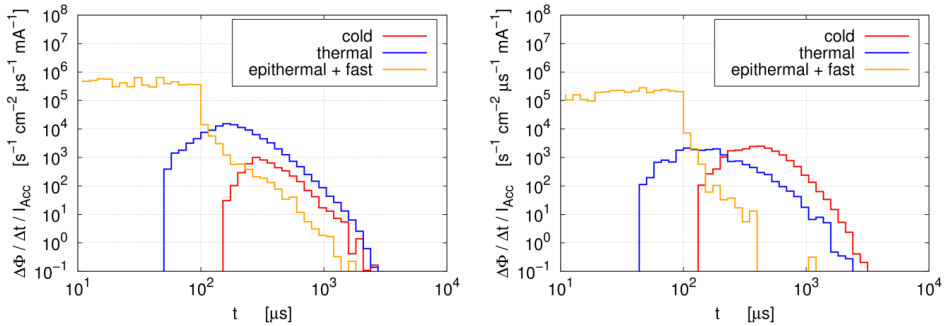


Fig. A3.3. The time structure of fast, thermal and cold neutron pulses delivered by the thermal neutron channel T3 (left) and the cold neutrons channel C3 with solid methane as cold moderator (right) (see Fig. 3.12 for corresponding beam-line configuration). The beryllium target is used for production of fast neutrons. The length of the proton pulse is 100 μs .

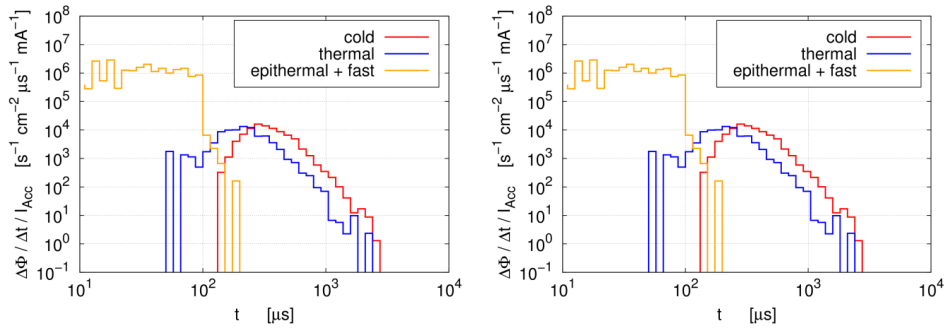


Fig. A3.4. The time structure of fast, thermal and cold neutron pulses delivered by the fast neutron channel F1 (left) and the cold neutrons channel C4 with liquid parahydrogen as cold moderator (right) (see Fig. 3.12 for corresponding beam-line configuration). The beryllium target is used for production of fast neutrons. The length of the proton pulse is μs .

Table A3.1. Full width at half maximum (FWHM) of neutron pulses and die-away-times of thermal and cold neutrons for the neutron channels (see Fig. 3.12 for corresponding beam-line configuration). The beryllium target is used for production of fast neutrons. The length of the proton pulse is 100 μs Λ_1 and Λ_2 are the short and long component of the die-away-time.

	Thermal neutrons pulse			Cold neutrons pulse		
	FWHM (μs)	Λ_1 (μs)	Λ_2 (μs)	FWHM (μs)	Λ_1 (μs)	Λ_2 (μs)
Configuration a						
T1	165(17)	129(3)	243(12)	188(19)	-	-
T2	170(16)	104(2)	161(3)	214(219)	-	-
C1	155(16)	118(15)	222(15)	384(38)	244(5)	-
C2	181(18)	100(4)	185(11)	252(25)	164(5)	294(35)
Configuration b						
T3	167(17)	145(4)	270(6)	207(21)	-	-
C3	162(16)	125(30)	217(9)	384(38)	250(4)	-
C4	177(18)	122(12)	192(18)	261(26)	243(5)	204(8)
F1	181(18)	-	-	219(22)		

Appendix 4 Brilliance for the neutron channels

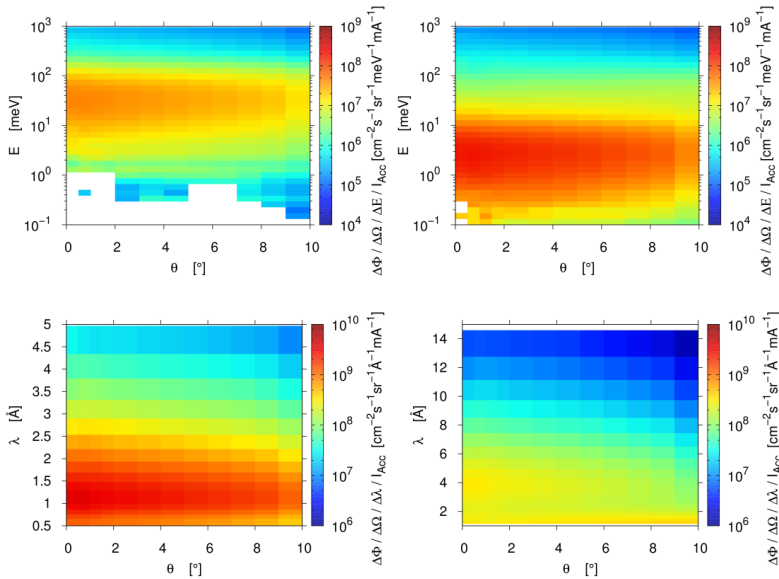


Fig. A4.1. Brilliance delivered by the thermal neutron channel T1 (left) and the cold neutron channel C1 with solid methane as cold moderator (right) at surface of lead reflector (see Fig. 3.12 for corresponding beam-line configuration). The beryllium target is used for the production of fast neutrons.

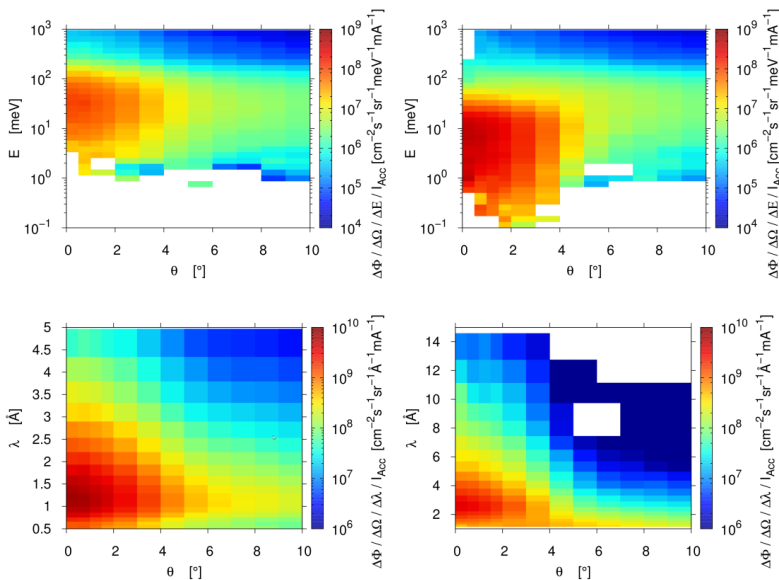


Fig. A4.2. Brilliance delivered by the thermal neutron channel T2 (left) and the cold neutron channel C2 with liquid parahydrogen as cold moderator (right) (see Fig. 3.12 for corresponding beam-line configuration). The beryllium target is used for the production of fast neutrons.

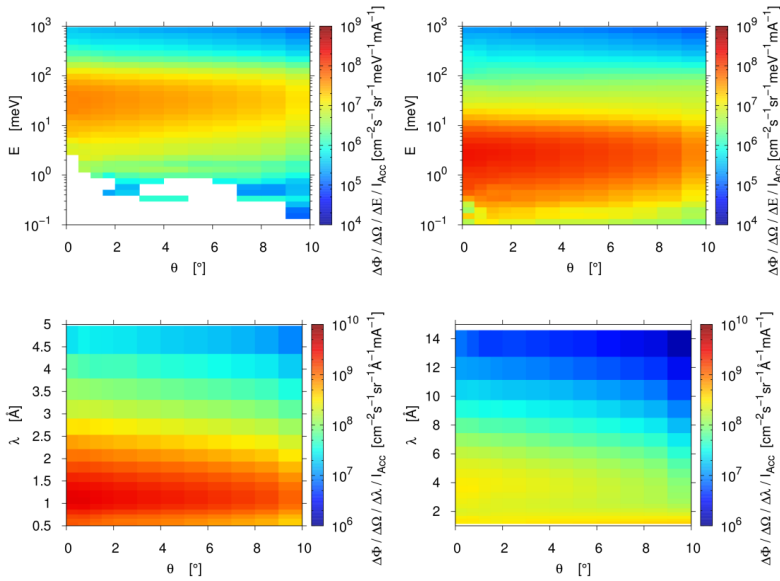


Fig. A4.3. Brilliance delivered by the thermal neutron channel T3 (left) and the cold neutron channel C3 with solid methane as cold moderator (right) (see Fig. 3.12 for corresponding beam-line configuration). The beryllium target is used for the production of fast neutrons.

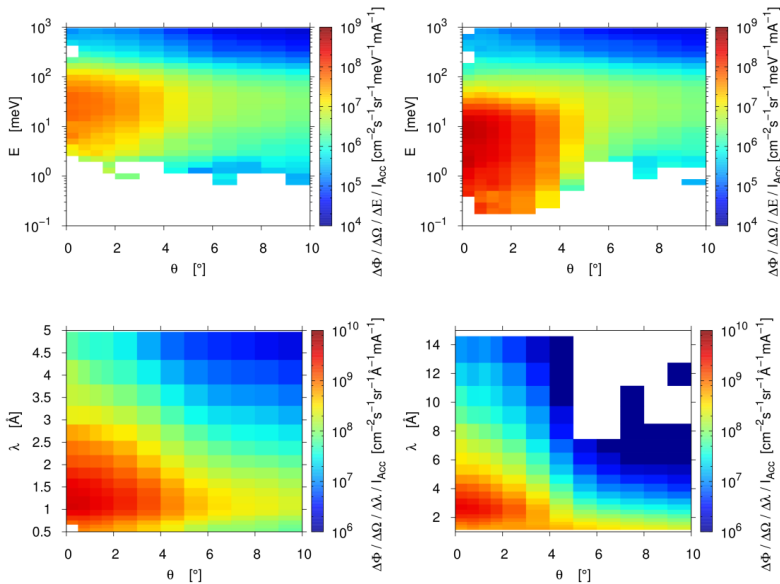


Fig. A4.4. Brilliance delivered by the fast neutron channel F1 (left) and the cold neutron channel C4 with liquid parahydrogen as cold moderator (right) (see Fig. 3.12 for corresponding beam-line configuration). The beryllium target is used for the production of fast neutrons.

Appendix 5 Excerpt (summarised) of the German radiation ordinance (StrlSchV) for installation and operation of a facility producing ionizing radiation

§ 11 Genehmigungsvoraussetzungen für den Betrieb von Anlagen zur Erzeugung ionisierender Strahlen

- (1) Wer eine Anlage zur Erzeugung ionisierender Strahlen der folgenden Art errichtet, bedarf der Genehmigung:
 1. Beschleuniger- oder Plasmaanlage, in der je Sekunde mehr als 10^{12} Neutronen erzeugt werden können
 4. Ionenbeschleuniger mit einer Endenergie der Ionen von mehr als 10 MeV je Nukleon, sofern die mittlere Strahlleistung 50 Watt übersteigen kann
- (2) Betrieb oder wesentliche Änderung einer Anlage zur Erzeugung ionisierender Strahlen bedarf der Genehmigung

§ 12 Anzeigebedürftiger Betrieb von Anlagen zur Erzeugung ionisierender Strahlen

- (1) Betrieb und wesentliche Änderung des Betriebs, Inbetriebnahme soll der zuständigen Behörde schriftlich angezeigt werden.
 2. Eines Ionenbeschleunigers, bei dessen Betrieb die Ortsdosisleistung von 10 Mikrosievert durch Stunde im Abstand von 0.1 Meter von der berührbaren Oberfläche nicht überschritten wird
- (2) Der Behörde ist auf Verlangen nachzuweisen, dass die für die sichere Ausführung des Betriebs notwendige Anzahl von SSB vorhanden ist.

§ 13 Genehmigungsvoraussetzungen für die Errichtung von Anlagen zur Erzeugung ionisierender Strahlen

Die Genehmigung nach § 11 ist zu erteilen, wenn

1. Keine Bedenken über die Zuverlässigkeit des Antragstellers vorliegen,
2. ein SSB bestellt wird, der über die nötige Fachkunde und Zuverlässigkeit verfügt,
3. die Strahlenexposition in allgemeinen zugänglichen Bereichen der Anlage sowie außerhalb der Anlage die zugelassenen Werte nicht überschreitet. Ableitung radioaktiver Stoffe mit Luft und Wasser und die austretende gestreute Strahlung ist zu berücksichtigen,
4. Vorschriften über den Schutz der Umwelt bei dem beabsichtigten Betrieb der Anlage sowie bei Störfällen eingehalten werden können,
5. der erforderliche Schutz gegen Störmaßnahmen oder sonstige Einwirkungen Dritter gewährleistet ist,
6. Überwiegende öffentliche Interessen im Hinblick auf die Umweltauswirkungen bei beabsichtigten Betrieb der Anlagen nicht entgegenstehen.

§ 14 Genehmigungsvoraussetzungen für den Betrieb von Anlagen zur Erzeugung ionisierender Strahlen

1., 2. wie §13

4. gewährleistet ist, dass die bei dem Betrieb sonst tätigen Personen die notwendigen Kenntnisse über die mögliche Strahlengefährdung und die anzuwendenden Schutzmaßnahmen besitzen,
5. gewährleistet ist, dass bei dem Betrieb die Ausrüstungen vorhanden und die Maßnahmen getroffen sind, die nach dem Stand von Wissenschaft und Technik erforderlich sind, damit die Schutzvorschriften eingehalten werden,
8. der erforderliche Schutz gegen Störmaßnahmen oder sonstige Einwirkungen Dritter gewährleistet ist.

Appendix 6 Activity Calculation

The activity of the radionuclides induced by proton and neutron interactions with the beryllium target, the vanadium target and the aluminium mounting is shown in the following figures.

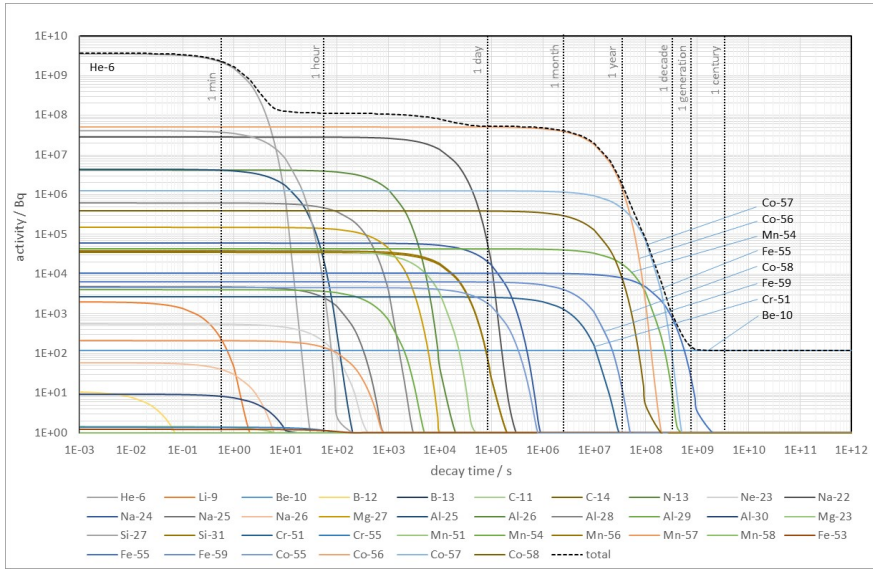


Fig. A6.1. Decay of the radionuclides formed by proton and neutron activation in the beryllium target ($m = 6.5 \text{ g}$) during 2,000 h of operation without interruption

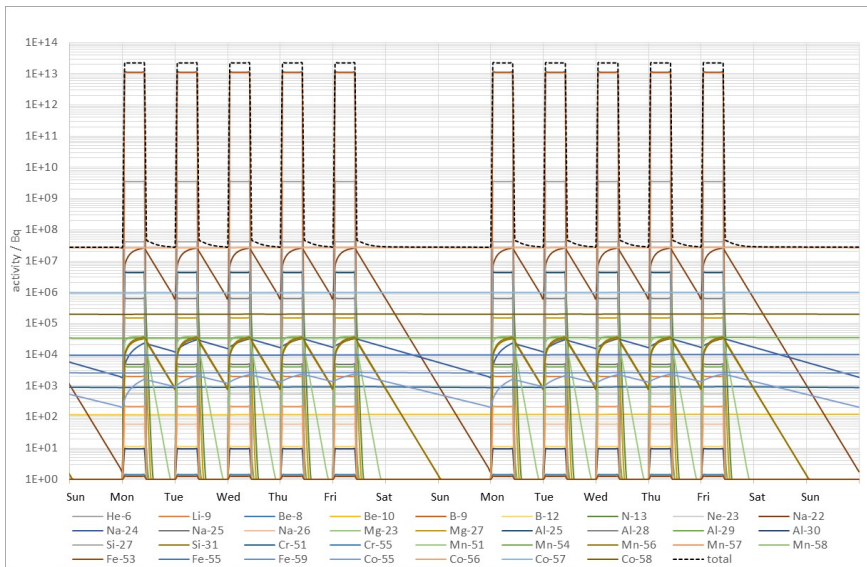


Fig. A6.2. Activity of the radionuclides formed by proton and neutron activation in the beryllium target ($m = 6.5 \text{ g}$) at week 39 and 40 out of 40 weeks of irradiation with 10 h of irradiation per working day and 5 working days per week (in total 2,000 h of irradiation)

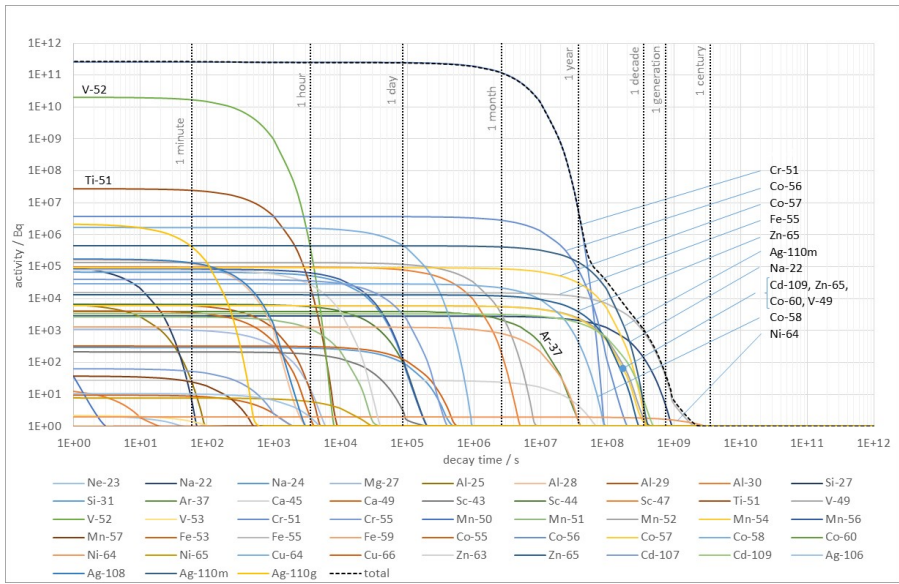


Fig. A6.3. Decay of the radionuclides formed by proton and neutron activation in the vanadium target ($m = 61.4\text{ g}$) during 2,000 h of operation without interruption

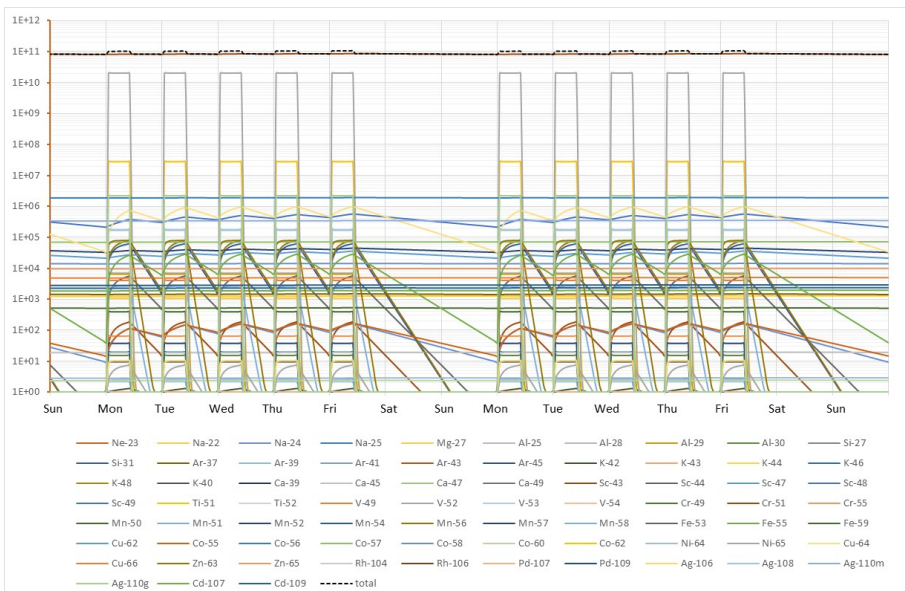


Fig. A6.4. Activity of the radionuclides formed by proton and neutron activation in the vanadium target ($m = 61.4\text{ g}$) at week 39 and 40 out of 40 weeks of irradiation with 10 h of irradiation per working day and 5 working days per week (in total 2000 h of irradiation)

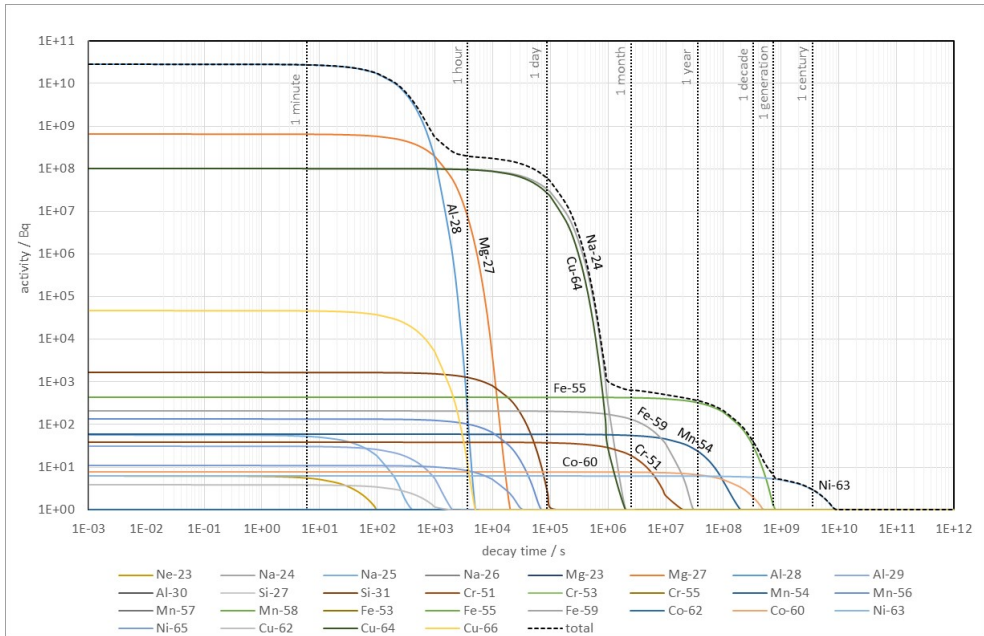


Fig. A6.5. Decay of the radionuclides formed by neutron activation in the aluminum mounting ($m = 1,100$ g) during 2,000 h of operation without interruption

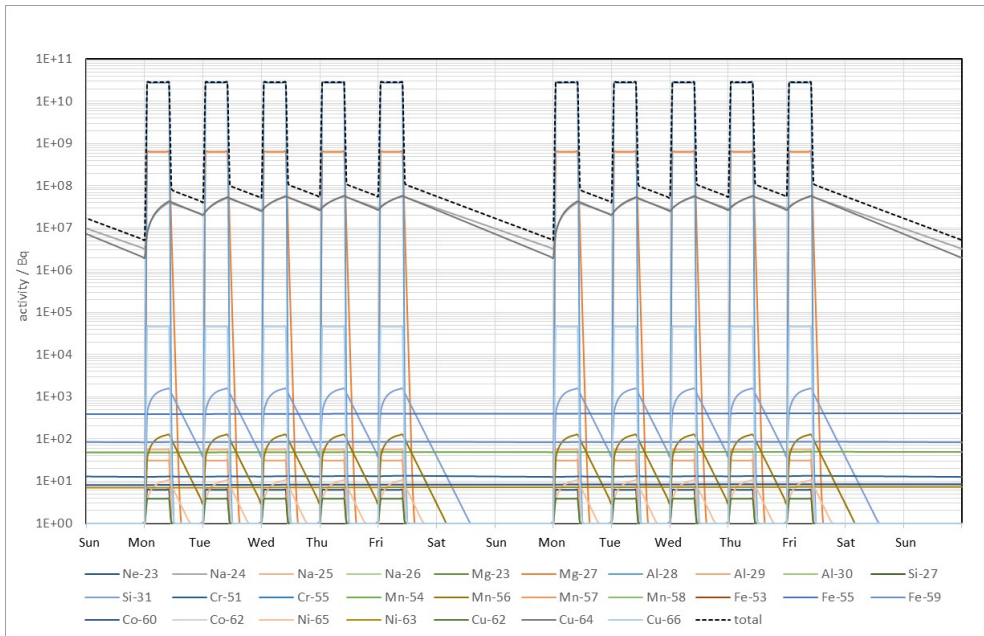


Fig. A6.6. Activity of the radionuclides formed by neutron activation in the aluminum mounting ($m = 1,100$ g) at week 39 and 40 out of 40 weeks of irradiation with 10 h of irradiation per working day and 5 working days per week (in total 2000 h of irradiation)

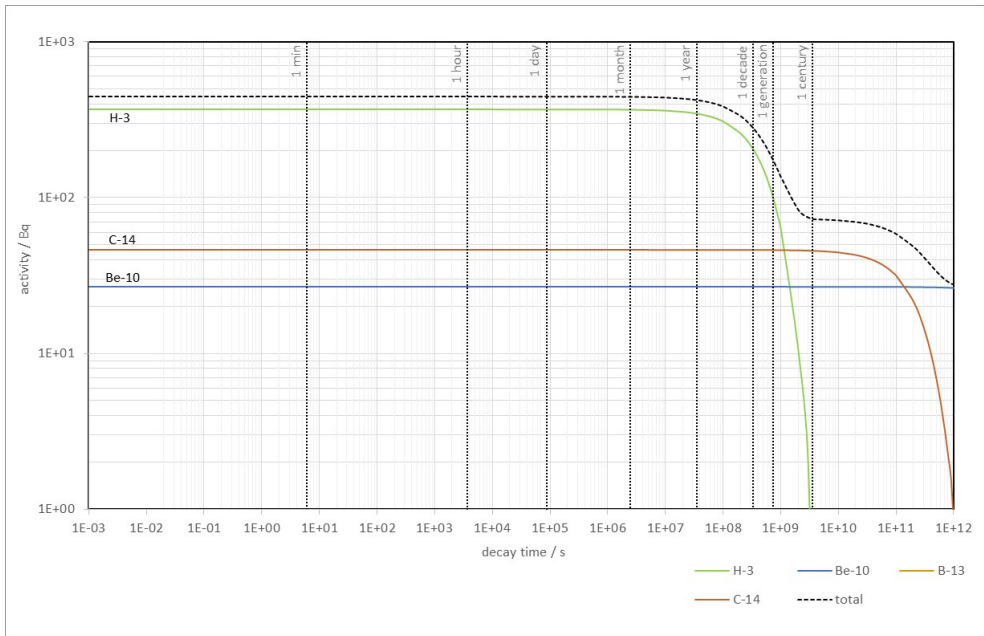


Fig. A6.7. Decay of the radionuclides formed by neutron activation in the polyethylene moderator ($m = 1,300 \text{ g}$) during 2,000 h of operation without interruption

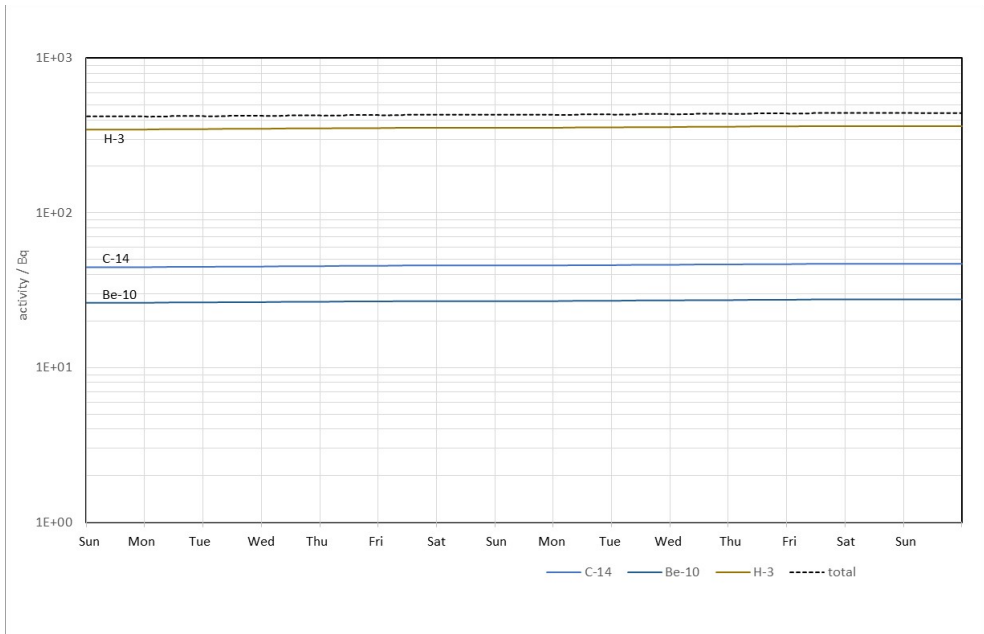


Fig. A6.8. Activity of the radionuclides formed by neutron activation in the polyethylene moderator ($m = 1,300 \text{ g}$) at week 39 and 40 out of 40 weeks of irradiation with 10 h of irradiation per working day and 5 working days per week (in total 2,000 h of irradiation)

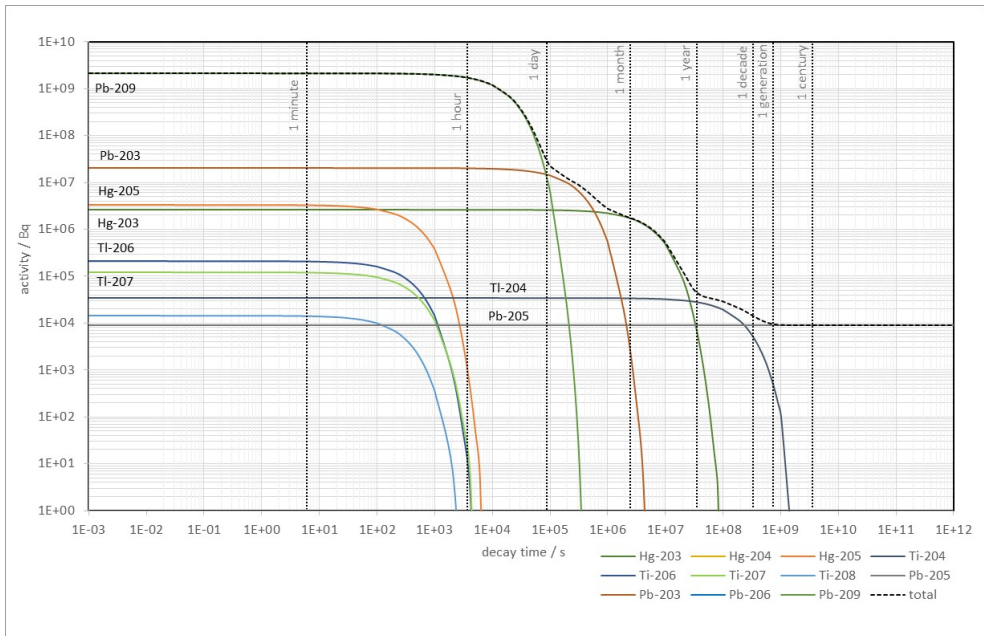


Fig. A6.9. Decay of the radionuclides formed by neutron activation in the lead reflector ($m = 1,000 \text{ kg}$) during 2,000 h of operation without interruption

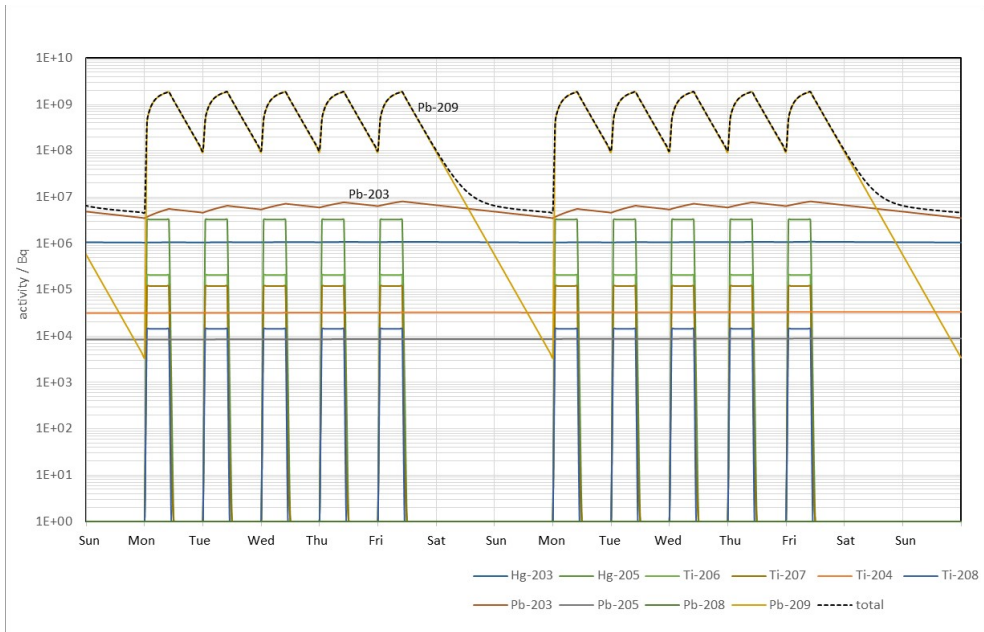


Fig. A6.10. Activity of the radionuclides formed by neutron activation in the lead reflector ($m = 1,000 \text{ kg}$) at week 39 and 40 out of 40 weeks of irradiation with 10 h of irradiation per working day and 5 working days per week (in total 2,000 h of irradiation)

Band / Volume 1

Fundamentos de Ensaio de Vazamento e Estanqueidade

J. da Cruz Payão Filho, W. Schmidt, G. Schröder (2000), 340 pp
ISBN: 3-89336-278-9

Band / Volume 2

Nur das Geld zählt? Erfassung von Nutzenorientierungen bei der Zuteilung von Geld und materiellen Gütern

M. Ertinger (2003), 333 pp
ISBN: 3-89336-336-X

Band / Volume 3

Advances in Nuclear and Radiochemistry

Extended Abstracts of Papers presented at the Sixth International Conference on Nuclear and Radiochemistry (NRC-6), 29 August to 3 September 2004, Aachen, Germany

edited by S. M. Qaim, H. H. Coenen (2004), XXXII, 794 pp
ISBN: 3-89336-362-9

Band / Volume 4

Wissenschaft im Zeichen der Zeit

Preisträger des Leibfried-Preises im Forschungszentrum Jülich 2000 – 2005
herausgegeben von R. Ball (2005), ca. 185 pp
ISBN: 3-89336-411-0

Band / Volume 5

Proceedings of the 1st International Conference on Natural and Biomimetic Mechanosensing

edited by: J. Casas, G. Krijnen, M. Malkoc-Thust, J. Mogdans, A. Offenhäusser, H. Peremans (2009), ca. 80 pp
ISBN: 978-3-89336-583-8

Band / Volume 6

Leo Brandt (1908-1971)

Ingenieur – Wissenschaftsförderer – Visionär

Wissenschaftliche Konferenz zum 100. Geburtstag des nordrhein-westfälischen Forschungspolitikers und Gründers des Forschungszentrums Jülich
herausgegeben von B. Mittermaier, B.-A. Rusinek (2009), I, 121 pp
ISBN: 978-3-89336-602-6

Band / Volume 7

Conceptual Design Report

NOVA ERA

(Neutrons Obtained Via Accelerator for Education and Research Activities)

A Jülich High Brilliance Neutron Source project

E. Mauerhofer, U. Rücker, T. Cronert, P. Zakalek, J. Baggemann, P.-E. Doege, J. Li,
S. Böhm, H. Kleines, T. Gutberlet, and T. Brückel (2017), 68 pp

ISBN: 978-3-95806-280-1

**Allgemeines /
General
Band / Volume 7
ISBN 978-3-95806-280-1**

